

EDDY HEAT FLUXES AT DRAKE PASSAGE
DUE TO MESOSCALE MOTIONS

A Thesis
by
RICARDO LUIS ROJAS RECABAL

Submitted to the Graduate College of
Texas A&M University
in partial fulfillment of the requirement for the degree of

MASTER OF SCIENCE

May 1982

Major Subject: Oceanography

EDDY HEAT FLUXES AT DRAKE PASSAGE
DUE TO MESOSCALE MOTIONS

A Thesis
by
RICARDO LUIS ROJAS RECABAL

Approved as to style and content by:

Worth D. Nowlin Jr

(Chairman of Committee)

Michael Longnecker

(Member)

John M. Klinck

(Member)

Robert O. Keif

(Member)

Robert O. Keif

(Head of Department)

May 1982

1805701

ABSTRACT

Eddy Heat Fluxes at Drake Passage

Due to Mesoscale Motions. (May 1982)

Ricardo Luis Rojas Recabal, B.S., Catholic University

of Valparaiso, Chile

Chairman of Advisory Committee: Dr. Worth D. Nowlin, Jr.

Heat budget studies have shown that a net poleward heat flux across the Antarctic Circumpolar Current (ACC) is required to balance the heat lost by the sea to the atmosphere around Antarctica. This study investigates the contribution to the heat flux across the ACC which can be attributed to correlations between mesoscale fluctuations in temperature and fluctuations in the north-south velocity component. The data base consists of 9-to 12-month current and temperature records from 47 current meters distributed on 22 subsurface moorings spanning Drake Passage.

Unlike previous data sets, the 1979 records included pressure measurements to monitor the vertical displacements of the instruments as large horizontal speeds caused the mooring configuration to depart from the vertical, or to blow-over. A careful study was made of the error in eddy heat flux which results if no correction to the temperature time series is made to compensate for mooring blow-over. It is shown that the use of an uncorrected temperature time series results in over-estimating the poleward heat flux by

approximately 30%. A method of correcting the temperature time series for blow-over using recorded pressures and historical vertical temperature gradients was developed.

The resulting estimates show bands of poleward and equatorward eddy heat flux across Drake Passage. This pattern results from aliasing of the calculations due to single or multiple long-term events in the records. It is shown that the removal of such long-term events by separating the records into several pieces before calculating eddy heat fluxes reduces the poleward heat flux and eliminates the equatorward heat flux. The remaining poleward eddy heat fluxes were shown to be dominated by individual events. For most records individual mesoscale fluctuations contributed more than 50% of the record length heat flux in time periods constituting less than 20% of the total record lengths. The average eddy heat flux from our deep records across Drake Passage is 4.8 kWm^{-2} poleward, in good agreement with Bryden's (1979) estimate of 6.7 kWm^{-2} , considering that his estimates were not corrected for mooring blow-over.

ACKNOWLEDGEMENTS

After two years of graduate studies at Texas A&M University, I have so many people to whom to express my gratitude that the list of their names would not fit on this page. I only want to name some of them--the people who played an important role in this thesis research.

I wish to thank my advisory committee: Dr. W. D. Nowlin, Jr., Professor Robert O. Reid, Dr. John M. Klinck and Dr. Michael T. Longnecker for reviewing the manuscript and offering many helpful comments and suggestions.

I also want to thank the people from the ISOS group at Texas A&M University for their friendship and encouragement. Special thanks go to Dr. Thomas Whitworth III. His interest, dedication, encouragement and moral support are sincerely appreciated. Thanks to Steve Worley for helping me with the solution of computing problems. I am grateful to Elaine Hansen who typed many drafts of this thesis.

Finally, I have no words to express my gratitude to my committee chairman, Worth Nowlin, whose advice, interest, encouragement, patience and guidance have been a real support during my graduate studies at Texas A&M, specially during my darkest hours. His efforts can not be repaid.

TABLE OF CONTENTS

| | |
|--|------|
| ABSTRACT | iii |
| ACKNOWLEDGEMENTS | v |
| LIST OF TABLES | vii |
| LIST OF FIGURES | viii |
| INTRODUCTION | 1 |
| 1. Background | 1 |
| 2. Objectives of this Study | 8 |
| OBSERVATIONS AND METHODS | 10 |
| 1. Data Coverage | 10 |
| 2. Calculations | 10 |
| RESULTS OF RECORD-LENGTH EDDY HEAT FLUX CALCULATIONS | 26 |
| DISCUSSION OF RESULTS | 35 |
| 1. The 1979 Flow Field | 35 |
| 2. Influence of a Single Frontal Shift | 37 |
| 3. Influence of Individual Events | 59 |
| SUMMARY AND CONCLUSIONS | 75 |
| REFERENCES | 79 |
| APPENDIX | 81 |
| VITA | 130 |

LIST OF TABLES

| Table | Page |
|--|------|
| 1. Summary of pressure variations (in db) for DRAKE 79 meters which experienced the largest depth excursions. | 18 |
| 2. Historical vertical temperature gradients (r) for each of the four zones at Drake Passage (in 10^{-4} °C/db). | 20 |
| 3. Poleward, record-length eddy heat fluxes, Q , with statistical confidence estimates from DRAKE 79 data. | 27 |
| 4. Results from analysis of temperature and eddy heat flux for the uppermost meter at NT mooring shown in Fig. 6. \bar{T} and \bar{Q} are the record-length mean temperature and eddy heat flux for each case. . . . | 67 |

LIST OF FIGURES

| Figure | | Page |
|--------|---|------|
| 1. | Potential temperature ($^{\circ}\text{C}$) across the Antarctic Circumpolar Current at Drake Passage as observed in January 1979 as part of DRAKE 79. | 4 |
| 2. | Location of DRAKE 79 year-long moorings and of hydrographic stations occupied during deployment cruise of R/V MELVILLE. . . . | 11 |
| 3. | Vertical configuration for year-long moorings during DRAKE 79 (after Whitworth <i>et al.</i> , 1982). | 12 |
| 4. | Record-length mean values of meridional eddy heat flux, in kWm^{-2} , as a function of latitude and depth for the current meters on the Main Line. | 31 |
| 5. | Record-length mean values of meridional eddy heat flux, in kWm^{-2} , as a function of position and depth for the MS array. | 32 |
| 6. | Time history of 500-m isotherms along Main Line in Drake Passage as constructed from subjective analysis (Whitworth and Gallo, 1981). | 36 |
| 7.a. | Daily values of meridional velocity component for the upper meter at ML7. | 38 |
| 7.b. | Daily values of temperature for the upper meter at ML7. | 39 |
| 7.c. | Daily values of meridional eddy heat flux for the upper meter at ML7. | |
| 8.a. | Daily values of meridional velocity component for the intermediate depth meter at ML6. . . . | 42 |
| 8.b. | Daily values of temperature for the intermediate depth meter at ML6. | 43 |
| 8.c. | Daily values of meridional eddy heat flux for the intermediate depth at ML6. | 44 |

| Figure | | Page |
|--------|---|------|
| 9.a. | Daily values of meridional velocity component for the first part of the record from the intermediate depth meter at ML6. | 45 |
| 9.b. | Daily values of temperature for the first part of the record from the intermediate depth meter at ML6. | 46 |
| 9.c. | Daily values of meridional eddy heat flux for the first part of the record from the intermediate depth meter at ML6. | 47 |
| 10.a. | Daily values of meridional velocity component for the second part of the record from the intermediate depth meter at ML6. | 48 |
| 10.b. | Daily values of temperature for the second part of the record from the intermediate depth meter at ML6. | 49 |
| 10.c. | Daily values of meridional eddy heat flux for the second part of the record from the intermediate depth meter at ML6. | 50 |
| 11.a. | Daily values of meridional velocity component for the first part of the record from the upper meter at ML7. | 52 |
| 11.b. | Daily values of temperature for the first part of the record from the upper meter at ML7. | 53 |
| 11.c. | Daily values of meridional eddy heat flux for the first part of the record from the upper meter at ML7. | 54 |
| 12.a. | Daily values of meridional velocity component for the second part of the record from the upper meter at ML7. | 55 |
| 12.b. | Daily values of temperature for the second part of the record from the upper meter at ML7. | 56 |
| 12.c. | Daily values of meridional eddy heat flux for the second part of the record from the upper meter at ML7. | 57 |
| 13. | Temperature at 509 m on Mooring SS1000 during 1979. | 58 |

| Figure | | Page |
|--------|---|------|
| 14. | Daily average, meridional eddy heat flux for the meter at NS500. | 60 |
| 15.a. | Daily values of meridional eddy heat flux for the uppermost meter at mooring NT from original time series for entire record length. | 63 |
| 15.b. | Daily values of meridional eddy heat flux for the uppermost meter at NT using temperature time series at 647 m constructed from thermistor chain data to correct for mooring blow-over. Heavy curve shows cumulative mean eddy heat flux. | 64 |
| 15.c. | Daily values of meridional eddy heat flux for the uppermost meter at mooring NT from original time series with portion containing ring passage removed. | 65 |
| 15.d. | Daily values of meridional eddy heat flux for the uppermost meter at mooring NT from time series with portion containing ring passage removed and corrected in temperature for mooring blow-over. | 66 |
| 16.a. | Daily values of meridional velocity component for mooring NT at 949 m. | 69 |
| 16.b. | Daily values of temperature for mooring NT at 949 m. | 70 |
| 16.c. | Daily values of meridional eddy heat flux for mooring NT at 949. | 71 |
| 17.a. | Daily values of meridional velocity component for mooring ML1 at 810 m. | 72 |
| 17.b. | Daily values of temperature for mooring ML1 at 810 m. | 73 |
| 17.c. | Daily values of meridional eddy heat flux for mooring ML1 at 810 m. | 74 |
| A.1. | Daily average, meridional eddy heat flux for the instrument located at 533 m average depth on mooring NS500. Heavy line is cumulative mean eddy heat flux. | 83 |

| Figure | | Page |
|--------|---|------|
| A.2. | Daily average, meridional eddy heat flux for the instrument located at 528 m average depth on mooring NS1000. | 84 |
| A.3.a. | Daily average, meridional eddy heat flux for the instrument located at 647 m average depth on mooring NT. | 85 |
| A.3.b. | Daily average, meridional eddy heat flux for the instrument located at 944 m average depth on mooring NT. | 86 |
| A.3.c. | Daily average, meridional eddy heat flux for the instrument located at 1356 m average length on mooring NT. | 87 |
| A.3.d. | Daily average, meridional eddy heat flux for the instrument located at 1659 m average depth on mooring NT. | 88 |
| A.3.e. | Daily average, meridional eddy heat flux for the instrument located at 2650 m average depth on mooring NT. Heavy line is cumulative eddy heat flux. | 89 |
| A.4.a. | Daily average, meridional eddy heat flux for the instrument located at 810 m average depth on mooring ML1. Heavy line is cumulative eddy heat flux. | 90 |
| A.4.b. | Daily average, meridional eddy heat flux for the instrument located at 2733 m average depth on mooring ML1. | 91 |
| A.5.a. | Daily average, meridional eddy heat flux for the instrument located at 882 m average depth on mooring ML2. Heavy line is cumulative eddy heat flux. | 92 |
| A.5.b. | Daily average, meridional eddy heat flux for the instrument located at 2726 m average depth on mooring ML2. | 93 |
| A.6.a. | Daily average, meridional eddy heat flux for the instrument located at 647 m average depth on mooring ML5. | 94 |
| A.6.b. | Daily average, meridional eddy heat flux for the instrument located at 1351 m average depth on mooring ML5. | 95 |

| Figure | | Page |
|---------|--|------|
| A.6.c. | Daily average, meridional eddy heat flux for the instrument located at 2644 m average depth on mooring ML5. | 96 |
| A.7.a. | Daily average, meridional eddy heat flux for the instrument located at 689 m average depth on mooring ML6. | 97 |
| A.7.b. | Daily average, meridional eddy heat flux for the instrument located at 1391 m average depth on mooring ML6. | 98 |
| A.8.a. | Daily average, meridional eddy heat flux for the instrument located at 588 m average depth on mooring ML7. | 99 |
| A.8.b. | Daily average, meridional eddy heat flux for the instrument located at 1297 m average depth on mooring ML7. | 100 |
| A.8.c. | Daily average, meridional eddy heat flux for the instrument located at 2607 m average depth on mooring ML7. Heavy line is cumulative eddy heat flux. | 101 |
| A.9. | Daily average, meridional eddy heat flux for the instrument located at 610 m average depth on mooring ML8. | 102 |
| A.10. | Daily average, meridional eddy heat flux for the instrument located at 611 m average depth on mooring ML9. | 103 |
| A.11.a. | Daily average, meridional eddy heat flux for the instrument located at 500 m average depth on mooring ML10. | 104 |
| A.11.b. | Daily average, meridional eddy heat flux for the instrument located at 2590 m average depth on mooring ML10. | 105 |
| A.12. | Daily average, meridional eddy heat flux for the instrument located at 2658 m average depth on mooring ML11. | 106 |
| A.13.a. | Daily average, meridional eddy heat flux for the instrument located at 695 m average depth on mooring ST. | 107 |

| Figure | | Page |
|---------|---|------|
| A.13.b. | Daily average, meridional eddy heat flux for the instrument located on 1408 m average depth on mooring ST. | 108 |
| A.13.c. | Daily average, meridional eddy heat flux for the instrument located at 2715 m average depth on mooring ST. Heavy line is cumulative eddy heat flux. | 109 |
| A.14. | Daily average, meridional eddy heat flux for the instrument located at 509 m average depth on mooring SS1000. | 110 |
| A.15. | Daily average, meridional eddy heat flux for the instrument located at 500 m average depth on mooring SS500. | 111 |
| A.16.a. | Daily average, meridional eddy heat flux for the instrument located at 688 m average depth on mooring MS1. | 112 |
| A.16.b. | Daily average, meridional eddy heat flux for the instrument located at 1390 m average depth on mooring MS1. | 113 |
| A.16.c. | Daily average, meridional eddy heat flux for the instrument located at 2699 m average depth on mooring MS1. | 114 |
| A.17.c. | Daily average, meridional eddy heat flux for the instrument located at 804 m average depth on mooring MS2. | 115 |
| A.17.b. | Daily average, meridional eddy heat flux for the instrument located at 1493 m average depth on mooring MS2. | 116 |
| A.17.c. | Daily average, meridional eddy heat flux for the instrument located at 2785 m average depth on mooring MS2. | 117 |
| A.18. | Daily average, meridional eddy heat flux for the instrument located at 648 m average depth on mooring MS3. | 118 |
| A.19.a. | Daily average, meridional eddy heat flux for the instrument located at 500 m average depth on mooring MS4. | 119 |

| Figure | | Page |
|---------|---|------|
| A.19.b. | Daily average, meridional eddy heat flux for the instrument located at 2975 m average depth on mooring MS4. | 120 |
| A.20.a. | Daily average, meridional eddy heat flux for the instrument located at 755 m average depth on mooring MS5. | 121 |
| A.20.b. | Daily average, meridional eddy heat flux for the instrument located at 1468 m average depth on mooring MS5. | 122 |
| A.20.c. | Daily average meridional eddy heat flux for the instrument located at 2766 m average depth on mooring MS5. | 123 |
| A.21.a. | Daily average, meridional eddy heat flux for the instrument located at 819 m average depth on mooring MS6. | 124 |
| A.21.b. | Daily average, meridional eddy heat flux for the instrument located at 1416 m average depth on mooring MS6. | 125 |
| A.21.c. | Daily average, meridional eddy heat flux for the instrument located at 2709 m average depth on mooring MS6. | 126 |
| A.22.a. | Daily average, meridional eddy heat flux for the instrument located at 543 m average depth on mooring MS7. | 127 |
| A.22.b. | Daily average, meridional eddy heat flux for the instrument located at 1230 m average depth on mooring MS7. | 128 |
| A.22.c. | Daily average, meridional eddy heat flux for the instrument located at 2524 m average depth on mooring MS7. | 129 |

INTRODUCTION

1. Background

In this study new measurements are used to estimate heat fluxes across the Antarctic Circumpolar Current which flows through Drake Passage. The background given in this section provides a brief physical description of the waters which flow through Drake Passage and describes previous related work on heat flux.

a. The Antarctic Circumpolar Current System at Drake Passage

The ocean region between the southern tip of South America (Cape Horn) and the South Shetland Islands on the northernmost continental margin of the Antarctic Peninsula is known as Drake Passage. The width of the passage is approximately 800 km. Its average depth is near 3600 m, though there are trenches in the southern passage deeper than 5000 m and the topography in the northern passage is quite rough with hills and ridges rising to within 2000 m of the sea surface.

Drake Passage is the only major direct connection between the Atlantic and Pacific Oceans. Through the passage flows one of the world's largest ocean currents, the Antarctic Circumpolar Current (ACC), which circles the globe north of Antarctica flowing from west to east. The passage acts as a constriction to the flow; it is the narrowest channel through which the ACC must pass and is some 1000 to 1500 m shallower than the southeast Pacific or southwest

The style and format of this thesis conform to that of the *Journal of Physical Oceanography*.

Atlantic basins. The cross-passage orientation is MNW to SSE so that the average through-passage flow direction is to the ENE.

Much of the recent field work in Drake Passage has been carried out as part of the International Southern Ocean Studies (ISOS) program. A series of experiments called the First Dynamic Response and Kinematics Experiment (FDRAKE) began in 1975 and concluded in 1979-1980 with a major field program, DRAKE 79. These experiments form the basis of our current understanding of the ACC at Drake Passage, and those results pertinent to this study are presented here. A full description of the field programs may be found in the International Southern Ocean Studies Program Summary.

The flow through Drake Passage is concentrated in three fronts or regions of relatively large geostrophic flow which separate four distinct water mass zones. The fronts are regions of large horizontal property gradients between zones of generally more uniform property characteristics. The major features of the thermal field across Drake Passage are illustrated in Fig. 1 which shows a temperature section observed in January 1979 from the R/V MELVILLE on the initial cruise of DRAKE 79. In this section, the Subantarctic Zone (SAZ) is confined to the extreme northern portion of the Passage between the South American Continental slope and station 13. The temperature in the SAZ decreases monotonically with depth. The Subantarctic Front is the southern boundary of the SAZ. A different stratification characterizes the Antarctic Zone (AAZ) found between stations 9

and 3. Here a temperature minimum resulting from summer warming above the remnant of the cold, winter mixed layer dominates the upper water column. The northern extent of this cold subsurface layer (between stations 9 and 10) marks the location of the Polar Front.

Between the Polar Front and the Subantarctic Front is a region of transition between the stratification found in the Subantarctic and Antarctic Zones. As a transition region, the Polar Frontal Zone (PFZ) displays a wide variety of thermal stratification, ranging from the near-Subantarctic to the near-Antarctic. Fig. 1 also illustrates a transient feature frequently observed in Drake Passage, a cold-core ring of Antarctic water from south of the Polar Front which has separated from that water mass and become isolated within the PFZ. The ring, located between stations 14 and 15, represents one way in which heat can be transferred across the Polar Front. A second mechanism can be inferred from the temperature distribution north of the Polar Front between stations 10 and 17. Here, cold water from the Antarctic Zone sinks below the warmer surface waters of the PFZ resulting in a temperature profile with numerous inversions and reversals. These inversions, which characterize the process of interleaving, range in vertical scale from a few meters to tens of meters and are thought to be a major source of heat exchange across the Polar Front.

The southernmost zone in Drake Passage is the Continental Zone, which is separated from the Antarctic Zone by the Continental Water Boundary (between stations 2 and 3 in Fig. 1). The Continental Zone is distinct in its temperature/salinity relationship only at depths

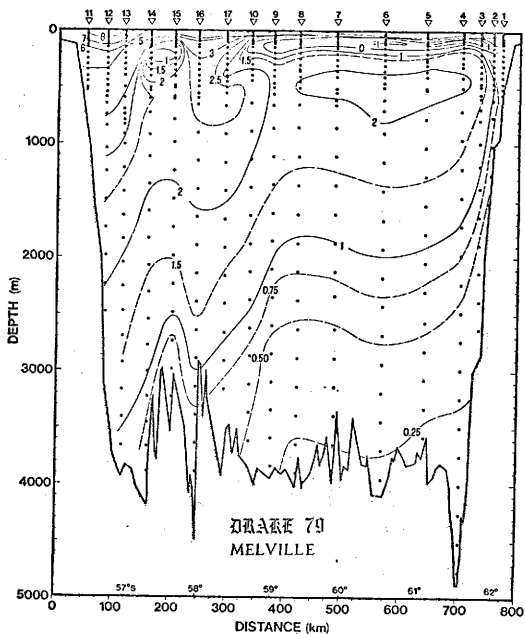


Fig. 1. Potential temperature ($^{\circ}\text{C}$) across the Antarctic Circumpolar Current at Drake Passage as observed in January 1979 as part of DRAKE 79.

above about 500 m. Below 500 m in the southern Passage and below ~2000 m in the north, a single water mass, the Circumpolar Deep Water (CDW) fills Drake Passage. Although the CDW has a nearly uniform T/S relationship, Nowlin et al. (1977) have shown that it reflects the surface zonation in its horizontal property gradients. This is seen in Fig. 1 as regions of large horizontal temperature gradients in the deep water at each front.

Surface speeds within the fronts are typically 30-40 cm/s and most of the transport through the Passage is in the frontal regions (Nowlin and Clifford, 1982). The velocities within the fronts are highly coherent vertically, and below the surface waters the vertical shear of current is remarkably uniform (Pillsbury et al., 1979). Meanderings of the Subantarctic and Polar Fronts frequently result in lateral shifts in frontal positions of up to 100 km in periods as short as a week (Nowlin et al., 1977). On two occasions during ISOS field work, meanders of the Polar Front have pinched off to produce isolated cold-core rings (Joyce and Patterson, 1977; Peterson et al., 1982). An understanding of the frontal movements during DRAKE 79 will prove to be crucial to the interpretation of the heat flux measurements presented in this study.

b. Heat flux; previous related work

Ever since the oceans were understood to play an important role in the earth's thermal balance, much emphasis has been given to heat transport by ocean currents. Previous studies on the role of ocean currents in transporting energy poleward have shown different mean meridional patterns for different oceans.

In the Northern Hemisphere, Vonder Harr and Oort (1973), using an indirect method combining satellite data on the net radiation budget of the earth-atmosphere system together with atmospheric energy transport estimates based on rawinsonde data, calculated that the oceanic role in the total poleward heat transport was important relative to that of the atmosphere only at low to middle latitudes. Using the same method Trenberth (1979) found that in the Southern Hemisphere the ocean heat transport was comparable in value to that of the atmosphere at higher latitudes (60°S), in contrast to the situation for the Northern Hemisphere, where the ocean transport seems negligible at higher latitudes. Gordon (1975) estimated poleward heat flux by the ocean to be about $4 \times 10^{14}\text{W}$ in order to compensate for the heat lost to the atmosphere south of the Polar Front. More recently Gordon (see deSzoeko and Levine, 1981) has reduced his estimated value to $3 \times 10^{14}\text{W}$.

deSzoeko and Levine (1981) presented an average heat balance for the Southern Ocean south of the Polar Front. They developed a method to calculate, using historical hydrographic data, the mean advective heat flux past a closed curve, near the mean position of the Polar Front, due to mean baroclinic and barotropic geostrophic motions within the interior oceans (excluding the surface and bottom boundary layer). They found no net meridional heat flux by mean advection within the ocean interior ($0 \pm 2.3 \times 10^{14}\text{W}$). However, they found an equatorward heat flow across the Polar Front of $1.5 \times 10^{14}\text{W}$ due to the surface wind-driven Ekman layer. Adding that Ekman flux to Gordon's estimate of heat lost to the atmosphere, they obtained a

value of $4.5 \times 10^{14} \text{W}$ for poleward heat flow in the ocean across the Polar Front which must be supplied by other processes. Possible candidates include northward flow of cold bottom water, small-scale processes such as interleaving across the Polar Front and heat flux due to mesoscale fluctuations. The latter is a strong candidate for the mechanism responsible for achieving the heat balance of the Southern Ocean.

In order to estimate the heat flux past a fixed location due to mesoscale fluctuations, time series of measurements of horizontal velocity and temperature are made at the location. The long term means are removed from the velocity components and temperature, and the flux of heat resulting from correlated fluctuations of temperature and speed along the axis of interest is estimated. This is called the eddy heat flux. If the original time series are filtered to remove high frequency fluctuations, then the resulting eddy heat flux is an estimate of heat flux due to phenomena with meso- and long-period fluctuations.

The first attempt to compute eddy heat fluxes across the ACC time series used were from 9 to 12 months long and were made during 1975 at depths near 2700 m on six moorings distributed more or less uniformly across Drake Passage between Cape Horn and the South Shetland Islands. Bryden (1979) estimated that the current and temperature fluctuations having periods greater than two days produce an average poleward eddy heat flux of 6.7 kWm^{-2} . Assuming these

values were typical of those throughout the water column over the entire circumpolar region this heat flux would be large enough to account for the entire poleward heat transport across the Polar Front estimated by Gordon.

A second evaluation of mesoscale eddy heat fluxes at Drake Passage was carried out by Sciremammano (1980). He extended Bryden's computations over a depth range from 300 to 3500 m using 1977 measurements from a cluster of 5 moorings in the central passage and for another year using 1976 measurements at three locations (northern, central and southern passage) which had been sampled also during 1975. The measured heat flux was large at the center of the passage as a result of mesoscale disturbances crossing the Polar Front (meanders, migration of the Front or eddies formed from it). In general, Sciremammano (1980) arrived at the same conclusion as Bryden (1979), i.e., the poleward heat flux due to low frequency motions is large at Drake Passage.

In addition to these mesoscale phenomena (rings, eddies or meanders) responsible for the eddy heat flux estimated by Bryden (1981), other phenomena have been shown to be important in the transfer of heat across the Polar Front, namely small-scale, cross-frontal intrusions or interleaves (Joyce and Patterson, 1977; Joyce et al., 1978).

2. Objectives of this Study

The nature and magnitude of the meridional oceanic flux of heat across the Antarctic Circumpolar Current are important to our understanding of the oceanic heat budget and climate. Based on a

very limited number of measurements, previous studies have indicated that eddy heat fluxes across this current are (1) poleward, (2) due principally to mesoscale processes and (3) significant in terms of balancing the sea-to-atmosphere heat exchange occurring of the Circumpolar Current. During 1979, temperature and velocity were measured hourly at a large number of locations spanning the Circumpolar Current at Drake Passage. From these measurements new estimates of eddy heat flux can be made and their significance to meridional heat exchange in the ocean estimated.

The first objective of this study is to correct the 1979 measurements in Drake Passage for sampling problems so that reasonably accurate, Eulerian time series of temperature and horizontal velocity are available from which to compute heat fluxes. The second objective is to determine a methodology for obtaining reasonable estimates of meridional eddy heat flux associated with mesoscale events from the time series. A third objective is to extend spatially the previous eddy heat flux estimates to provide wider coverage of Drake Passage through more intensive synoptic measurements during 1979. The final general objective is to compare with previous estimates the new heat flux estimates and to examine the implications of these estimates relative to the heat budget of the Southern Ocean.

OBSERVATIONS AND METHODS

1. Data Coverage

Horizontal current and temperature records from 47 current meters distributed on 22 subsurface arrays moored in Drake Passage were obtained during the DRAKE 79 experiment. The moorings were deployed during January and February of 1979 and recovered in February of 1980; most records are nearly one year long. Figure 2 shows a plan view of the locations of the year-long moorings as well as the hydrographic stations occupied as part of the field program. Fifteen moorings were on the Main Line across the passage from Cape Horn to Hero Bay in the South Shetland Islands; the remaining seven moorings were in the central passage west of that line in what is referred to as Mapping and Statistics (MS) array. The vertical distribution of instruments is pictured in Fig. 3 which also indicates data recovery.

2. Calculations

Values of poleward, eddy heat flux for the i th day are computed using the relation (after the work of Reynolds, 1894),

$$Q_i = \bar{\rho} C_p (v'T')_i, \quad (1)$$

where $\bar{\rho}$ and C_p are the mean density and specific heat of seawater respectively, daily meridional velocity and temperature values are given by

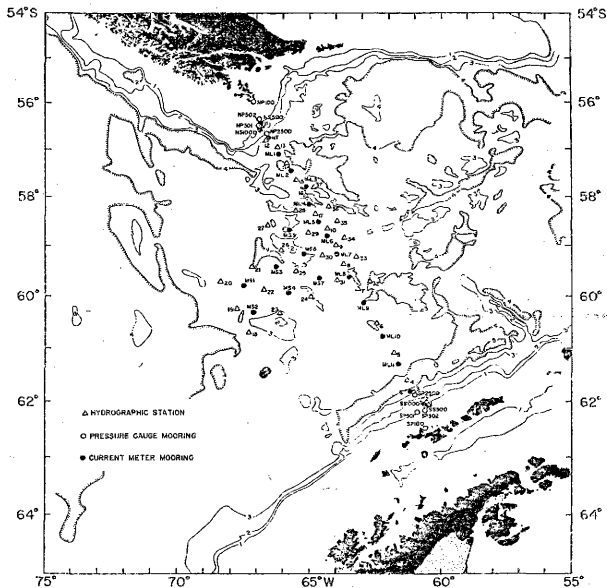


Fig. 2. Location of DRAKE 79 year-long moorings and of hydrographic stations occupied during deployment cruise of R/V MELVILLE.

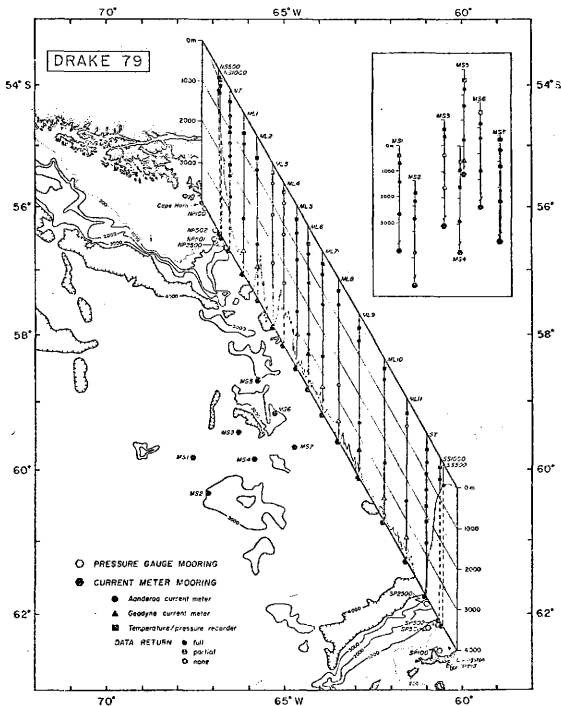


Fig. 3. Vertical configuration for year-long moorings during DRAKE 79 (after Whitworth *et al.*, 1982). Data recovery is also shown.

$$\begin{aligned}v &= \bar{v} + v', \\T &= \bar{T} + T',\end{aligned}\tag{2}$$

where v is the meridional component of velocity (taken positive when northward), with bars denoting record-length (time) averages and primes denoting turbulent (random) fluctuations of each variable about its mean value. The mean poleward, eddy heat flux component for each current meter is obtained by

$$Q \equiv \rho C_p \overline{v'T'} = \rho C_p n^{-1} \sum_{i=1}^n (v'T')_i,\tag{3}$$

where n is the total record length, in days.

The data, originally sampled at one-hour intervals, were low-pass filtered with a (60 + 1 + 60 point) cosine-Lanczos filter with a half-power point at 40 hours. The filtered series were resampled at a 6-h intervals. Since this filtering smooths the data over a period longer than one day (Pillsbury *et al.*, 1979), no loss of information is expected if daily averages are formed. In this study daily values of all variables are used, obtained by averaging four 6-h values.

The low-pass filtering of the original time series removes from the subsequent heat flux estimates all contributions due to phenomena manifested as fluctuations with periods shorter than a few days. Contributions from phenomena with fluctuations as sensed at a fixed location, of all longer periods to a maximum period equal to the record length are included in the heat flux estimates.

a. Corrections for depth excursions of instruments

In order to compute an eddy heat flux representative of a special spatial position, time series of v and T at a fixed point are required. If the moorings to which the recording instruments are attached move about in time, T and v vary as functions of time and depth (and to a lesser extent of horizontal position which is neglected here).

Glass floats were distributed along the mooring line above the instrument packages to provide buoyancy on the moorings used in the DRAKE 79 array. In order to increase the chances of survival for long periods in a hostile environment the moorings were designed to be "soft", that is with relatively little reserve buoyancy. With such a design the moorings yield or "blow over" during a strong current event rather than move their anchors, as might be the case for a mooring on which the buoyancy almost equals the weight of mooring and anchor, a "stiff" mooring.

The blow-over of a mooring in the presence of strong currents gives rise to difficulties in analyzing and interpreting the records obtained from instruments on the mooring, since we generally desire time series at fixed positions. Thus it is necessary to correct the time series for depth, or pressure, excursions encountered by the instruments, if it is believed that such excursions will alias the interpretation of the data.

An error is introduced when estimating $\overline{v'T'}$ by using directly the measured velocity and temperature time series rather than attempting to correct the velocity and temperature values to a

constant depth. Since little is known about the time dependent vertical profiles of horizontal velocity, no correction has been attempted. It should be noted, however, that geostrophic shear profiles indicated only small corrections would be needed. Since information regarding the spatial distribution of temperature in Drake Passage is available, corrections can be made to the temperature time series to remove (or at least diminish) the effects of blow-over.

The special configuration of the upper part of the North Transport (NT) mooring allowed the accurate reconstruction of a temperature time series at a fixed depth corresponding to the average depth of the uppermost meter. On this mooring were four Aanderaa 100-m thermistor chains: three above the uppermost meter and one below. These gave the vertical distribution of temperature as a function of time over a pressure interval which included the record-length average pressure of the current/temperature recorder. The pressure at each thermistor bead on the chain was calculated from a knowledge of pressure at the current meter and at the T/P recorder above the thermistor chains under the assumption that pressure differences along the mooring varied linearly as mooring line length. A new time series of temperature at the mean pressure was constructed by selecting at each time the temperature at the appropriate depth from the thermistor chain data.

The value of $\overline{V'T'}$ calculated using this corrected temperature time series was compared to that calculated from the uncorrected temperature time series (obtained at the time-dependent depth of the meter). The mean eddy heat flux from the uncorrected time series

was 96.1 kWm^{-2} , poleward, whereas that from the corrected time series was only 67.7 kWm^{-2} , a reduction of almost 30% from the uncorrected value. I expected the poleward, eddy heat flux to be exaggerated by mooring blow-over since the vertical excursions of the meter allow the sensors to record lower temperatures than the actual values at the mean depth considered because of the vertical temperature stratification (decreasing temperature with increasing depth). If the vertical excursion during blow-over is large, the resulting lower temperatures will bias the mean record-length temperature, resulting in a record-length mean which is too low to represent accurately the average temperature at the mean depth of the meter.

Since the dense temperature measurements on NT were unique to that mooring, an alternative method of correcting other DRAKE 79 temperature records for blow-over was required. The temperature records from the remaining DRAKE 79 instruments were corrected for blow-over using historical vertical temperature gradients by the relation

$$T_{ci} = T_i + r (\bar{P} - P_i) \quad (4)$$

where T_{ci} is the *i*th corrected temperature value; T_i is the *i*th observed temperature value; r is the historical temperature gradient appropriate to the water mass zone and pressure range for the instrument; P_i is pressure recorded with T_i ; and \bar{P} is the pressure to which temperature is to be corrected, taken as the record-length mean for the instrument.

Pressure records were available from most current meters and were used to make the corrections. However, there were some meters which were driven off scale by large vertical excursions. Extreme examples are the deep meter at ML1, for which the pressure records are missing during 14% of the record length, and both upper and deep meters at ML2, for which pressure values are missing are 9% and 3% of their record lengths, respectively. For some meters no pressure records were obtained; the meter at SS500; the upper meter at MS4; and the deep meters at ML5, MS2, MS4, MS6 and MS7. The correction for blow-over applied to records from these meters is discussed later in this section. In Table 1 are summarized some of the largest pressure variations recorded during the experiment.

The historical temperature gradients were computed for two pressure ranges within each water mass zone. They are presented in Table 2. The temperature vs. pressure profiles used to compute these gradients were compiled by Whitworth (1979) from all the useful data available in a period of almost 50 years. These profiles were used under the assumption that they better represent each zone than would profiles from specific cruises. That historical data from different years can be averaged is supported by work of Nowlin and Clifford (1982) who find remarkable uniformity in vertical profiles of T, S and O_2 within each zone from year to year and from cruise to cruise.

As shown in Table 2, the vertical temperature gradients for different zones have markedly different values in the upper layers. To correct properly the temperatures at a specific mooring, detailed

Table 1. Summary of pressure variations (in db) for DRAKE 79 meters which experienced the largest depth excursions.

| Mooring | Mean | Max. | Min. | Range | Var. | S.D. |
|---------|--------|--------|--------|-------|---------|-------|
| NT | 647.8 | 981.7 | 598.1 | 383.6 | 3790.7 | 61.6 |
| NT | 948.9 | 1235.7 | 910.3 | 325.5 | 2540.3 | 50.4 |
| ML1 | 810.0 | 1331.1 | 481.4 | 849.7 | 44490.8 | 210.9 |
| ML1 | 2732.6 | 2972.3 | 2556.7 | 415.5 | 14523.3 | 120.5 |
| ML2 | 882.2 | 1417.1 | 571.3 | 845.8 | 29196.1 | 170.9 |
| ML2 | 2725.6 | 2958.5 | 2568.4 | 390.1 | 6615.5 | 81.3 |
| ML6 | 688.8 | 1034.8 | 624.7 | 410.1 | 5858.9 | 76.5 |
| ML6 | 1391.4 | 1683.6 | 1337.5 | 346.1 | 4227.8 | 65.0 |
| ML7 | 587.9 | 899.9 | 506.9 | 392.9 | 8343.9 | 91.3 |
| ML7 | 1297.0 | 1566.0 | 1234.4 | 331.6 | 5976.7 | 77.3 |

knowledge of which zone the mooring was in as a function of time would be required. Where frontal shifts past a mooring are frequent, the application of different corrections would be impractical. We avoid the problem near the Polar Front since upper-layer temperature gradients for the PFZ and AAZ are nearly the same. Similarly, since the deep layers of the Passage are of one water mass (CDW) the distinction is unnecessary as shown by the similar values of r in the northern three zones. Because the SAF frequently moved past the positions of Moorings ML1 and ML2, they were sometimes in the SAZ and sometimes in the PFZ. This movement of the front past the moorings caused the upper meters to experience depth excursions outside the depth range used to calculate the vertical temperature gradients for upper layers given in Table 2. Thus, for correcting temperatures at the upper meters on ML1 and ML2 special r values of $-19.5 \times 10^{-4} \text{ }^{\circ}\text{C/db}$ and $-4.50 \times 10^{-4} \text{ }^{\circ}\text{C/db}$ were calculated from historical data. Fortunately, the moorings at the extreme northern and southern boundaries of the Passage remain in one zone for the entire year.

To test this method of correcting temperature for instrument blow-over, the mean eddy heat flux was computed using the mean gradient correction for the uppermost meter at NT and compared with results obtained by correcting temperature using the thermistor data. The mean eddy heat flux for the temperature time series corrected using the historical temperature gradient ($-20.8 \times 10^{-4} \text{ }^{\circ}\text{C/db}$; upper SAZ) gave a value of 69.8 kWm^{-2} poleward, a difference of 3% compared to the value of 67.7 kWm^{-2} poleward heat flux obtained

Table 2. Historical vertical temperature gradients (γ) for each of the four zones at Drake Passage (in $10^{-4} \text{ }^{\circ}\text{C/db}$). Standard errors are shown within square brackets.

| Layer/Zone | Subantarctic | Polar Frontal | Antarctic | Continental |
|----------------------------------|-----------------|-------------------|------------------|-----------------|
| Upper (= 500 to 1400 db) | -20.8 [0.93] | -3.83* [0.92] | -4.06* [0.55] | -5.16 [1.81] |
| Deeper (= 1000 to 3000 db) | -6.75 [0.24] | -6.62** [0.10] | -6.55 [0.21] | -3.59 [0.30] |

*The average value used for upper meters within the PFZ or AAZ was $3.95 \text{ }^{\circ}\text{C/db}$.

**The average value which was used for deeper meters within the SAZ, PFZ and AAZ.

from thermistor chain corrections. This current meter experienced some of the largest depth excursions recorded during DRAKE 79. Of course, it may be fortuitous that the mean values of eddy heat flux obtained using the two correction methods agreed so well. Nevertheless, this small difference provides some justification for use of the historical temperature gradient method in correcting the temperature time series to constant depths.

For those meters which produced no pressure records a constant correction factor was applied to the corresponding uncorrected mean eddy heat flux. The procedure is illustrated by considering the correction for the deepest meter at MS6. The corrected mean eddy heat flux was obtained by reducing the uncorrected value by 10%, i.e., using a correction factor of 0.9. This correction was selected after calculating the ratio $(\overline{v'T'})_c (\overline{v'T'})^{-1}$ for both shallower meters on the same mooring, where $(\overline{v'T'})_c$ is the corrected mean eddy heat flux (i.e., temperature corrected for mooring blow-over) and $\overline{v'T'}$ is the mean eddy heat flux from original records. The ratios for the upper (810 m) and intermediate (1416 m) meters were 0.90 and 0.93, respectively. Neither meter had a range of depth excursions larger than 100 m, and it can be assumed that the depth range for the deeper meter did not exceed 100 m. We further assume that a reduction of the value of $\overline{v'T'}$ by 10% will yield a reasonable estimate for $(\overline{v'T'})_c$ at the deepest meter. Similar procedures were used to obtain "corrected" values of eddy heat flux at the deep meters on ML5, MS2 and MS7. The uncorrected mean eddy heat flux was used at SS500 since the meter was located quite near the bottom and

little blow-over was possible. The uncorrected mean eddy heat fluxes were also used for both meters on mooring MS4, since neither had pressure records.

B. Error Estimates

Aanderaa current meters were used to measure and record temperature and water velocity. After calibration, the total errors in temperature and poleward component of velocity are not expected to exceed 0.04°C and 1 cm/s , respectively. Since such errors are expected to occur randomly and there is no reason to expect that poleward velocity and temperature errors would be correlated, they are not expected to influence estimates of eddy heat flux.

Apart from the measurement errors inherent in the instrumentation used, there are several potential sources of error associated with our measurements. One source of error is the use of mean (historical) vertical temperature gradients for the various water mass zones to correct the temperature time series for vertical excursions due to mooring blow-over. A simple linear regression model was applied to the historical data to obtain the best fit linear vertical temperature gradients (r) for each zone. In order to compare the fitted linear temperature gradients for each zone the standard error of the slope coefficients were computed (Ostle and Mensing, 1979). The standard error for each r estimate is

$$S_r = \left[\frac{\sum_{i=1}^n T_i - \hat{T}_i}{(n-2) \sum_{i=1}^n (P_i - \bar{P})^2} \right]^{1/2} \frac{^{\circ}\text{C}}{\text{db}} \quad (5)$$

where T_i is observed historical temperature at pressure P_i , \hat{T}_i is the temperature from the linear fit and \bar{P} is the mean pressure from the n observed values of T_i .

The largest errors are associated with the vertical temperature gradient within the PFZ. This is expected since the PFZ is a transition region representing a wide variety of thermal stratifications. We expect that the mean gradient minus the standard error would be representative of the southern PFZ while the mean gradient plus the standard error would best represent the northern portions of the PFZ. Moreover, since the Polar Front varies in position, we expect that any mooring near the front would sample a wide range of temperature gradients, and that the errors resulting from using a mean gradient would tend to cancel for year-long measurements.

As a check on a "worst case" error, the upper meters at moorings ML5 and ML6 were corrected with the mean gradient plus and minus the standard error. Using the mean temperature gradient ($-3.83 \times 10^{-4} \text{ } ^\circ\text{C/db}$) the eddy heat flux is -1.5 kWm^{-2} for ML5 at 647 m and -25.4 kWm^{-2} for ML6 at 688 m. The mean gradient plus the standard error ($-2.91 \times 10^{-4} \text{ } ^\circ\text{C/db}$) gave values of -2.3 kWm^{-2} for ML5 and 27.6 kWm^{-2} for ML6. The mean gradient minus the standard error ($-4.75 \times 10^{-4} \text{ } ^\circ\text{C/db}$) resulted in eddy heat fluxes of 0.6 kWm^{-2} for ML5 and -23.1 kWm^{-2} for ML6. Thus, even if the errors using the mean temperature gradient did not tend to cancel, the sign of the eddy heat flux would not change even though a large percentage of error at ML5 would result.

One important statistical consideration concerning the mean eddy heat flux is how much confidence we associate with the computation. By establishing the confidence interval about the mean eddy heat flux a statement of certainty may be made. This is especially important for small positive and negative heat fluxes, because these values may not be significantly different from zero.

The average observed heat fluxes are unbiased estimators of the true mean, μ . In order to account for the variation of the sample mean, a 95% confidence interval for μ was computed. There is 95% confidence that the true mean μ lies in the interval (U, L) given by

$$U = \bar{x} + t_{.975} (n-1) S_{\bar{x}}$$

and

(6)

$$L = \bar{x} - t_{.975} (n-1) S_{\bar{x}},$$

where:

\bar{x} = mean sample value, e.g., mean record-length eddy heat flux,

$$S_{\bar{x}} = s/\sqrt{n}$$

s = sample standard deviation,

n = number of data points,

r = % level of confidence (expressed as a fraction between 0-1) and

$t_{.975} (n-1)$ = 97.5% percentile of the "Student's t" distribution with n-1 degrees of freedom.

$S_{\bar{x}}^2$ is an estimator of the variance of \bar{x} , given by

$$\text{Var} (\bar{x}) = \frac{\sigma^2}{n} + \frac{2}{n^2} \sum_{i < j} \text{Cov} (x_i, x_j),$$

where x_i and x_j are daily average eddy heat flux values. If the covariances, $\text{Cov} (x_i, x_j)$, are zero then $S_{\bar{x}}^2$ is an unbiased estimator of $\text{Var} (\bar{x})$. If the covariances are positive, then $S_{\bar{x}}^2$ underestimates $\text{Var} (\bar{x})$ and the computed confidence intervals will be too narrow. On the other hand, if the covariances are negative, then $S_{\bar{x}}^2$ overestimates $\text{Var} (\bar{x})$ and the confidence intervals will have higher than 95% confidence. In the following calculations $S_{\bar{x}}$ will be used in order to simplify the calculations. The reader should thus be aware of the possible inaccuracy of these intervals as estimates of μ .

For each time series of daily eddy heat flux the record-length mean eddy heat flux was calculated. In order to estimate how this mean sample value represented the time series, calculations were made for each time series of the standard error, and confidence interval. In particular, each time series was tested to see whether the true mean differed from zero at the 95% confidence level, i.e., whether zero was outside the 95% confidence interval given by (6) around the record-length mean.

RESULTS OF RECORD-LENGTH EDDY HEAT FLUX CALCULATIONS

Record-length mean values of meridional eddy heat flux for all 1979 current meter records from Drake Passage have been computed using the methods described in the previous sections. In Table 3 are shown these heat flux values together with statistical confidence estimates, including standard deviation and upper and lower bounds as computed using equation 6. The statistical measures were calculated using daily heat flux values corrected for mooring blow-over for those meters which returned pressure records. For the following meters there were no usable pressure records: 2644 m at MLS, 500 m at SS500, 2785 m at MS2, 500 m and 2975 m at MS4, 2709 m at MS6 and 2524 m at MS7. At SS500 little vertical excursion was possible, and thus blow-over corrections were not necessary. To correct for blow-over at the other meters, heat flux values were multiplied by a factor near 0.9, as previously described. The values of standard deviations reported for those time series are from the uncorrected time series of $v'T'$. Thus, they are somewhat larger than would be the corresponding quantities from time series of $v'T'$ corrected for blow-over.

In the Appendix are presented the daily average of meridional eddy heat flux of the instrument records from the DRAKE 79 array. Also shown for each record is the cumulative mean of the heat flux as a function of time t given by:

Table 3. Poleward, record-length eddy heat fluxes, Q , with statistical confidence estimates from DRAKE 79 data. U and L are the upper and lower bounds for the true mean eddy heat flux at 95% confidence level. An asterisk denotes Q values which are not significantly different from zero at 95% confidence level.

| Mooring | Meter Depth (m) | Standard Deviation (kWm^{-2}) | U (kWm^{-2}) | Q (kWm^{-2}) | L (kWm^{-2}) |
|---------|-----------------|--|---------------------------|---------------------------|---------------------------|
| NS500 | 533 | 39.1 | -4.1 | -8.0 | -11.9 |
| NS1000 | 528 | 65.4 | -22.8 | -29.5 | -36.2 |
| NT | 647 | 161.7 | -43.4 | -67.7 | -92.0 |
| NT | 949 | 125.3 | -31.9 | -44.1 | -56.3 |
| NT | 1356 | 35.9 | 1.0 | -4.1* | -9.2 |
| NT | 1659 | 21.5 | -1.3 | -3.5 | -5.7 |
| NT | 2650 | 19.4 | -3.9 | -5.9 | -7.9 |
| ML1 | 810 | 207.2 | -91.6 | -111.6 | -136.4 |
| ML1 | 2733 | 33.7 | -3.7 | -7.0 | -10.3 |
| ML2 | 882 | 138.1 | -5.5 | -19.4 | -33.3 |
| ML2 | 2726 | 43.1 | -7.5 | -11.7 | -15.9 |
| ML5 | 647 | 87.6 | 7.3 | -1.3* | -9.9 |
| ML5 | 1351 | 39.9 | -2.6 | -5.9 | -9.2 |
| ML5 | 2644 | 20.2 | -2.1 | -4.3 | -6.5 |
| ML6 | 689 | 72.8 | -17.8 | -25.1 | -32.4 |
| ML6 | 1391 | 34.3 | -17.1 | -20.4 | -23.7 |
| ML7 | 588 | 42.9 | 31.9 | 27.4 | 22.9 |
| ML7 | 1297 | 23.3 | 15.0 | 12.7 | 10.4 |
| ML7 | 2607 | 16.1 | 1.2 | -0.4* | -2.0 |
| ML8 | 610 | 26.0 | 10.8 | 7.8 | 4.8 |

Table 3, Continued.

| Mooring | Meter Depth (m) | Standard Deviation (kWm^{-2}) | U (kWm^{-2}) | Q (kWm^{-2}) | L (kWm^{-2}) |
|---------|-----------------------|--|----------------------------|----------------------------|----------------------------|
| ML9 | 611 | 11.9 | 2.2 | 0.8* | -0.6 |
| ML10 | 500 | 32.4 | -4.6 | -7.7 | -10.8 |
| ML10 | 2590 | 8.6 | -0.4 | -1.2 | -2.0 |
| ML11 | 2658 | 11.6 | -2.9 | -4.1 | -5.3 |
| ST | 695 | 34.2 | -5.9 | -13.6 | -21.1 |
| ST | 1408 | 28.9 | 2.0 | -0.9* | -3.8 |
| ST | 2715 | 2.0 | 0.0 | -0.2 | -0.4 |
| SS1000 | 509 | 80.7 | 36.5 | 26.9 | 17.3 |
| SS500 | 500 | 54.7 | 18.0 | 12.5 | 7.0 |
| MS1 | 688 | 19.2 | 3.2 | 1.0* | -1.2 |
| MS1 | 1390 | 10.0 | 2.8 | 2.7 | 2.6 |
| MS1 | 2699 | 4.7 | 0.4 | 0.0* | -0.4 |
| MS2 | 804 | 13.2 | 6.7 | 5.3 | 3.9 |
| MS2 | 1493 | 9.1 | 3.9 | 3.8 | 3.7 |
| MS2 | 2785 | 5.9 | 3.2 | 2.6 | 2.0 |
| MS3 | 648 | 20.6 | -6.6 | -8.8 | -11.0 |
| MS4 | 500 | 12.4 | -4.0 | -5.6 | -7.2 |
| MS4 | 2975 | 5.5 | -0.2 | -0.8 | -1.4 |
| MS5 | 755 | 62.2 | 7.1 | 0.8* | -5.5 |
| MS5 | 1468 | 22.8 | 4.8 | 2.4* | 0.0 |
| MS5 | 2766 | 30.4 | 3.2 | 0.3* | -2.6 |
| MS6 | 819 | 31.9 | -7.8 | -11.1 | -14.4 |

Table 3, Continued

| Mooring | Meter Depth (m) | Standard Deviation (kWm^{-2}) | U (kWm^{-2}) | Q (kWm^{-2}) | L (kWm^{-2}) |
|---------|-----------------------|--|----------------------------|----------------------------|----------------------------|
| MS6 | 1416 | 25.9 | -8.1 | -10.8 | -13.5 |
| MS6 | 2709 | 19.6 | -4.5 | -6.5 | -8.5 |
| MS7 | 543 | 26.0 | 8.9 | 6.2 | 3.5 |
| MS7 | 1230 | 17.8 | 5.5 | 3.7 | 1.9 |
| MS7 | 2524 | 8.6 | 3.7 | 4.7 | 5.7 |

$$\bar{\rho} C_p m^{-1} \sum_{j=1}^m v'(j\Delta t) T'(j\Delta t)$$

at time $t = m\Delta t$.

Along the Main Line (Fig. 4) there is a poleward eddy heat flux at most locations, with the largest values in the northern passage. Near the central passage and near the southern continental boundary are zones in which the eddy heat fluxes are directed equatorward rather than poleward. This change in direction of flux is also found in the MS array (Fig. 5), in which most of the meters adjacent to moorings ML7 and ML8 show equatorward heat flux.

The general pattern is one of heat flux values decreasing with increasing depth in the water column. The sign of the heat flux is generally independent of depth. The pattern of depth dependence for the entire Drake Passage is in agreement with the high vertical coherence of both currents and temperature previously observed in specific areas of the passage (Pillsbury *et al.*, 1979; Sciremanmano *et al.*, 1980).

Eddy heat fluxes in Drake Passage are quite dependent on sampling locations and seem to be distributed in zones with large to moderate poleward values in the Subantarctic and Polar Frontal Zones respectively. In the northern part of the Antarctic Zone (just south of the Polar Front) a consistent equatorward heat flux is present throughout the water column, while poleward values are found in its southern part. In the Continental Zone the heat fluxes are moderately large and directed equatorward.

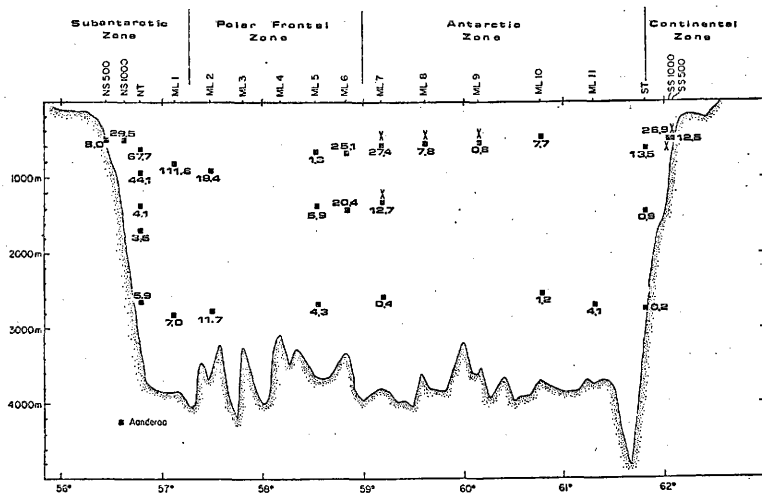


Fig. 4. Record-length mean values of meridional eddy heat flux, in kWm^{-2} , as a function of latitude and depth for the current meters on the Main Line. Fluxes are poleward unless marked with an x.

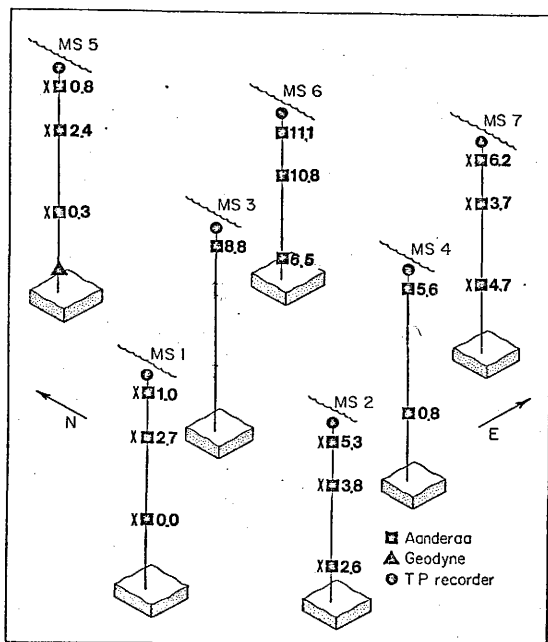


Fig. 5. Record-length mean values of meridional eddy heat flux, in kWm^{-2} , as a function of position and depth for the MS array. Fluxes are poleward unless marked with an x.

Spatial averages of eddy heat fluxes were computed to compare DRAKE 79 estimates with previous estimates. Heat fluxes for six deep records (2700 m) on the Main Line show an average poleward eddy heat flux of about 4.8 kWm^{-2} which is smaller than the value of 6.7 kWm^{-2} obtained by Bryden (1979) for FDRAKE 75 records. However, Bryden's records were not corrected for blow-over. The average of the original uncorrected heat flux values from the deep 1979 meters was 5.1 kWm^{-2} , which is closer to Bryden's value. The average value of eddy heat flux for the center of the passage for all depths greater than 1000 m was computed by Sciremammano (1980) from long-term records during 1975, 1976 and 1977. Although Sciremammano did not correct his values for mooring blow-over, his average value of 17 kWm^{-2} is considerably larger than that of 2.2 kWm^{-2} obtained for a subset of the 1979 current meters similarly located. The difference may be due in part to the large year-to-year variability found in this area, near the location of the Polar Front.

At most of the DRAKE 79 meters the true mean eddy heat flux is significantly different from zero at a 95% confidence level. The records from DRAKE 79 which do not meet this criterion are: NT at 1356 m, ML5 at 647 m, ML7 at 2607 m, ML9 at 611 m, ST at 1408 m, MS1 at 688 and 2699 m and the three meters at MS5. Those meters have mean eddy heat flux values very close to zero and/or large variances in the fluxes which makes the confidence bounds wide. The large variances are produced by events passing the moorings during the recording period.

Previous estimates of eddy heat flux from the ACC were all poleward. Thus, the present equatorward fluxes are unexpected. An explanation for this pattern of north-south zonation of heat fluxes was sought and is presented in the next chapter. First, the effects of long-term shifts past the moorings of thermal and kinematic structure is examined. This is followed by a discussion of the influence of mesoscale events (in the records) on the mean fluxes.

DISCUSSION OF RESULTS

1. The 1979 Flow Field

The three-dimensional character of the 1979 array permitted, for the first time in Drake Passage, a year-long description of the flow upstream of the central passage region. Weekly maps of temperature and velocity at the 500-m level were constructed from the instruments in the Mapping and Statistics Array and along the Main Line moorings (Whitworth and Gallo, 1981). Figure 6 shows the locations of the 500-m isotherms as a function of time across the Main Line moorings. The locations of the Subantarctic Front and the Polar Front can be roughly associated with the 3.5°C and the 2.3°C isotherms at this level. Two frequency ranges of frontal motions important to the understanding of eddy heat flux calculations are illustrated in this figure. The Subantarctic Front is highly variable in position with many aperiodic lateral shifts--probably associated with meanders in the front. Such meanders result in time series which are dominated by episodic variability as high speed current cores traverse the mooring location. Previous current measurements have shown the northern passage to be a region of extremely variable currents and temperatures (Nowlin *et al.*, 1980). Figure 6 shows frequent crossing of the Subantarctic Front past mooring ML2, for instance. During the first part of 1979, frontal crossings are so frequent that the time series may be too noisy to distinguish adequately individual events.

The Polar Front, by contrast, shows considerably less high frequency meandering on the Main Line. The entire year is dominated

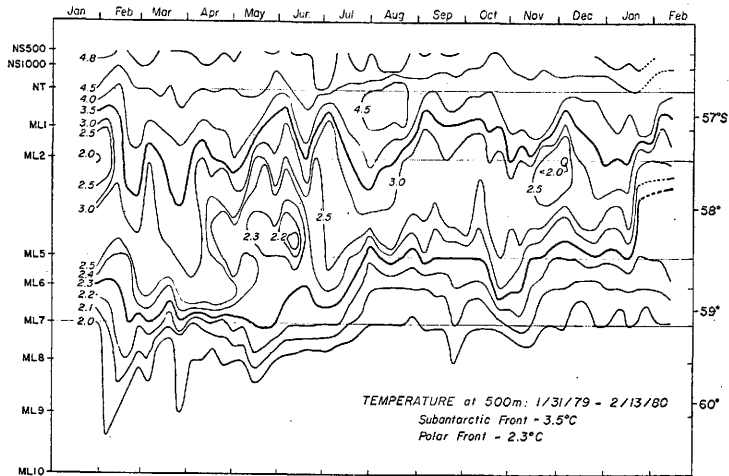


Fig. 6. Time history of 500-m isotherms along Main Line in Drake Passage as constructed from subjective analysis (Whitworth and Gallo, 1981).

by a single shift of the front from a southerly position to a more northerly one around mid-year. In the following two sections, the influence of these frequency ranges of events on eddy heat flux calculations will be assessed.

2. Influence of a Single Frontal Shift

The existence of eddy heat fluxes of opposite sign at moorings ML6 and ML7, less than 50 km apart, is unexpected. That the sign change occurs at all depths, is unaffected by corrections for mooring blow-over and also is supported by similar sign changes within the MS array is remarkable. In this section we will show that the anomalous equatorward heat flux at ML7 and the magnitude of the poleward heat flux at ML6 are both associated with the northward shift of the Polar Front which occurred in July 1979.

During the first half of the year the Polar Front was located close to the ML7 mooring which resulted in recorded fluctuation speeds larger than the record-length mean ($v' > 0$) and fluctuation temperature warmer than the record-length average ($T' > 0$). This combination produces equatorward eddy heat flux values over most of this portion of the record irrespective of correlations between mesoscale fluctuations in T and v . During the second half of the year the Polar Front was located north of the ML7 mooring, which resulted in speeds slower than average ($v' < 0$) and temperatures colder than average ($T' < 0$). This again produced equatorward eddy heat flux values, virtually independent of the correlation of mesoscale temperature and velocity fluctuations. This can be seen clearly in Fig. 7 where the plots of daily meridional velocity components,

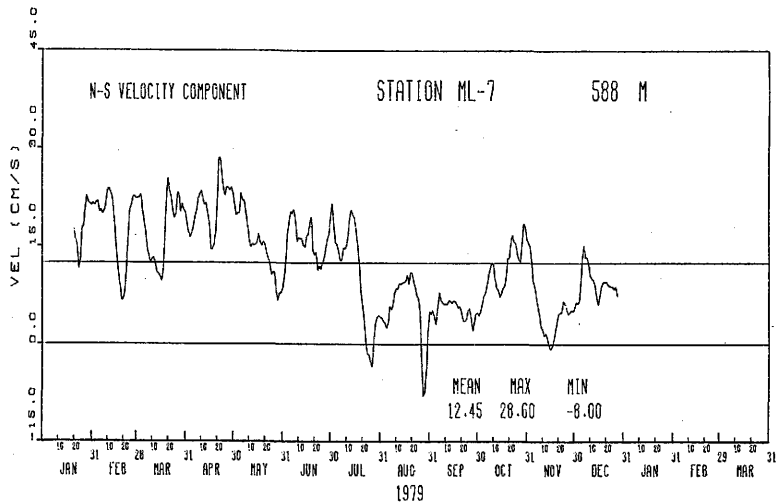


Fig. 7.a. Daily values of meridional velocity component for the upper meter at ML7.

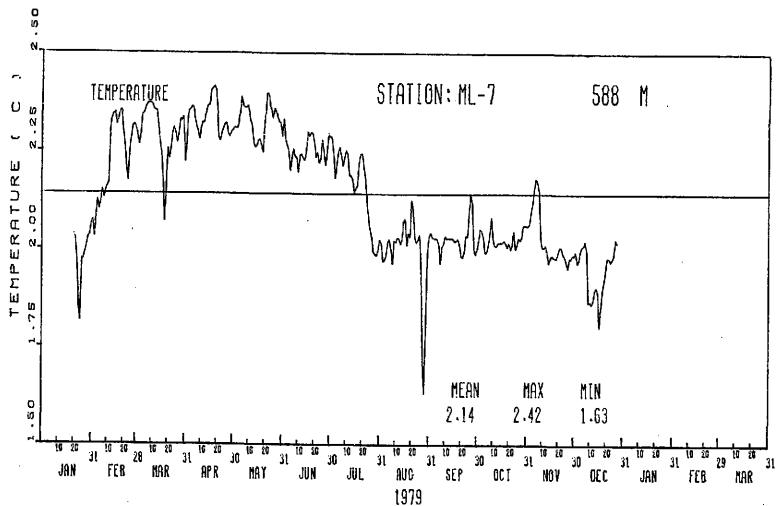


Fig. 7.b. Daily values of temperature for the upper meter at ML7.

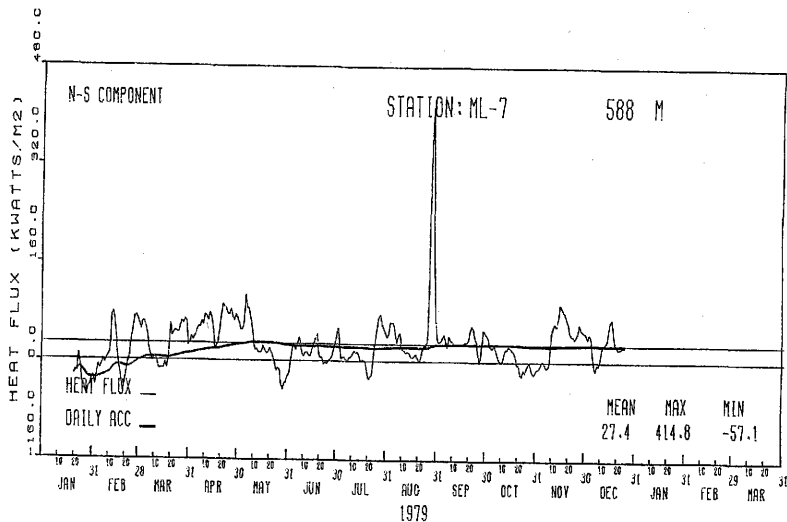


Fig. 7.c. Daily values of meridional eddy heat flux for the upper meter at ML7.

temperatures and eddy heat fluxes are presented for the uppermost meter. Other meters in the central passage which have equatorward mean eddy heat fluxes show similar patterns.

The same frontal shift produced the opposite effect immediately to the north at ML6. As shown in Fig. 8, a pattern similar to that at ML7 is present in the temperature fluctuations, but fluctuation velocities are primarily poleward for the first half year and equatorward for the second half. This combination of fluctuations results in a mean poleward eddy heat flux for the year.

The annual trend in the meandering of the Polar Front during 1979 could be due to the presence of a core cold ring in the central Drake Passage for the first half of the year (T. Whitworth III, personal communication). The single shift in location of the Polar Front influenced the velocity and temperature averages in such a way that the fluctuations we might expect from higher frequency eddy processes are completely masked by this large and long-term effect.

In order to illustrate the effect of the frontal shift, the original records for the uppermost meters at ML6 and ML7 were divided into two parts and the eddy heat fluxes computed for each segment. Temperatures, northward velocities and eddy heat fluxes from ML6 during the first and second halves of 1979 are shown in Figs. 9 and 10. The original poleward heat flux estimate of 20.4 kWm^{-2} is reduced by more than 50% by splitting the records into periods of warm and cold temperatures; the poleward heat flux is 1.4 kWm^{-2} during the first half of the year and 8.0 kWm^{-2} during the second half.

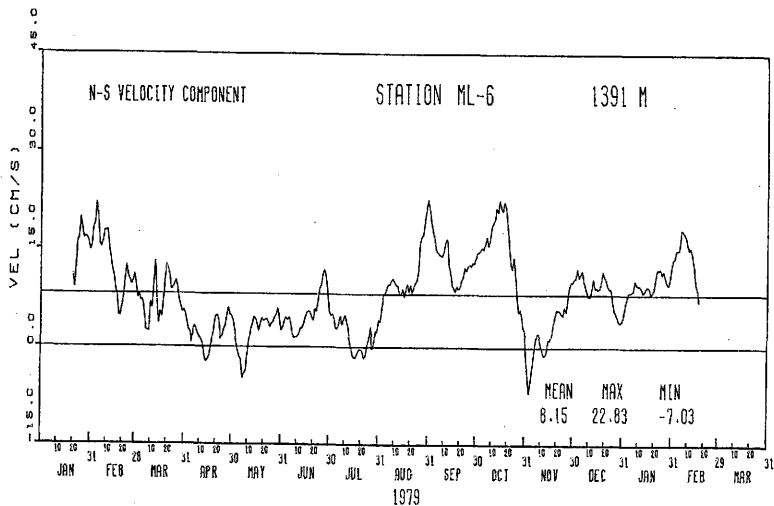


Fig. 8.a. Daily values of meridional velocity component for the intermediate depth meter at ML6.

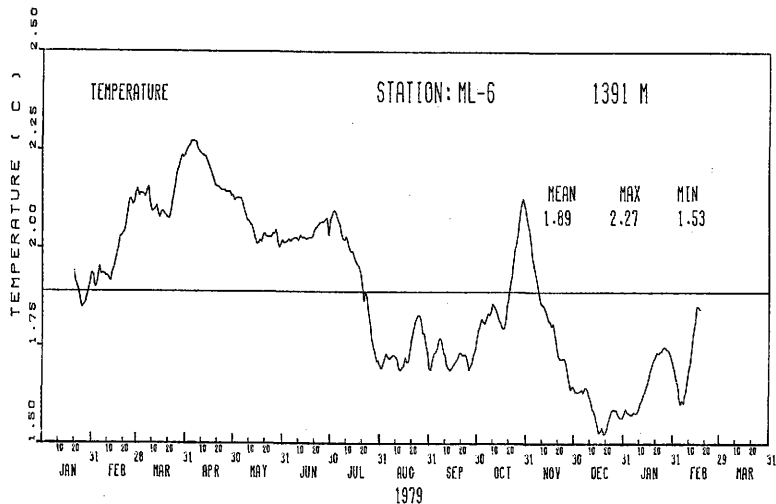


Fig. 8.b. Daily values of temperature for the intermediate depth meter at ML6.

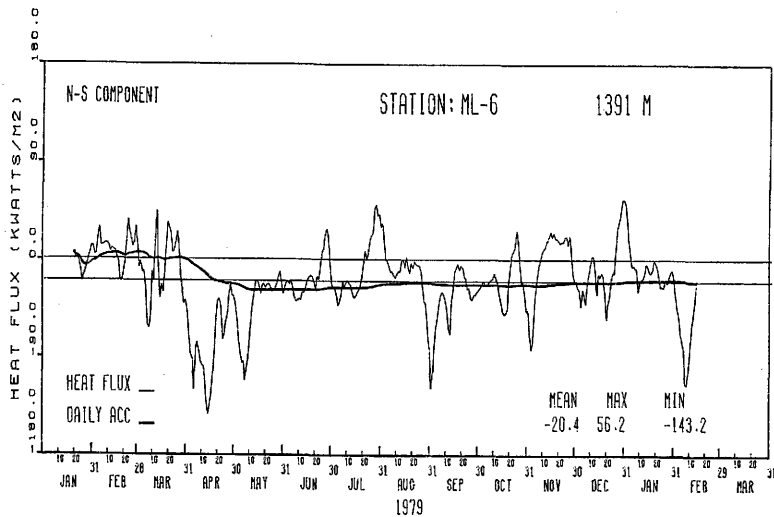


Fig. 8.c. Daily values of meridional eddy heat flux for the intermediate depth at ML6.

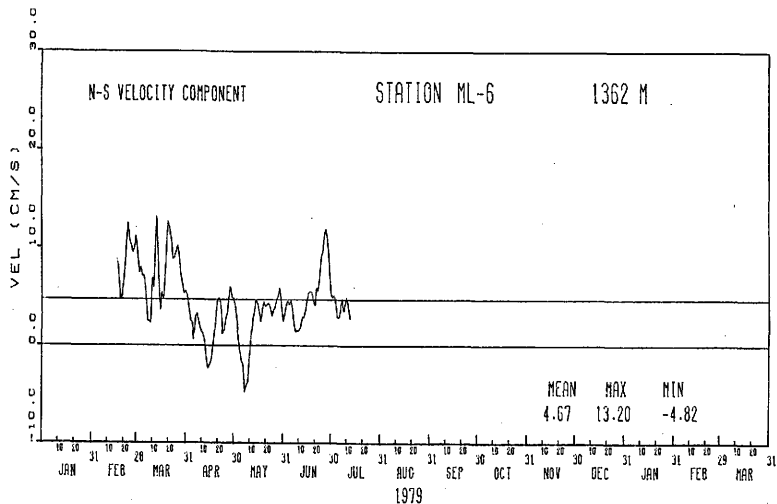


Fig. 9.a: Daily values of meridional velocity component for the first part of the record from the intermediate depth meter at ML6.

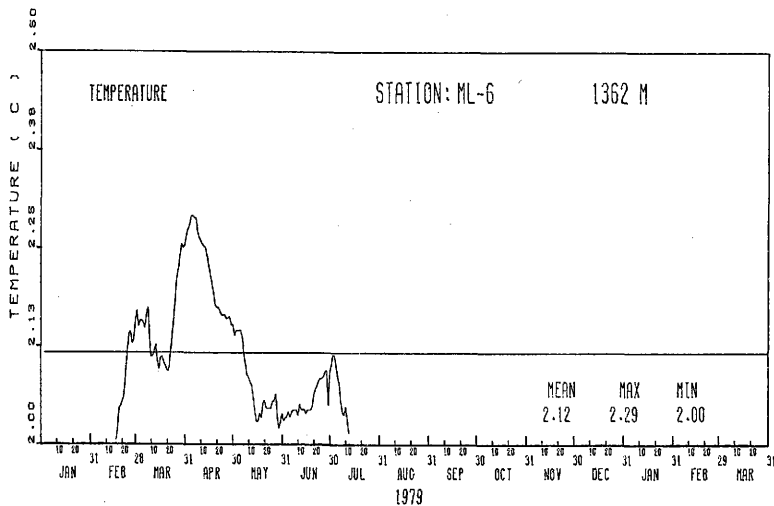


Fig. 9.b. Daily values of temperature for the first part of the record from the intermediate depth meter at ML6.

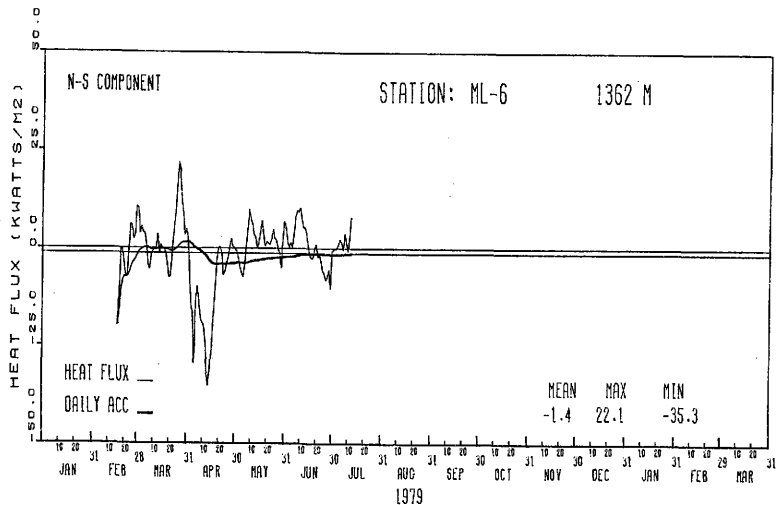


Fig. 9.c. Daily values of meridional eddy heat flux for the first part of the record from the intermediate depth meter at ML6.

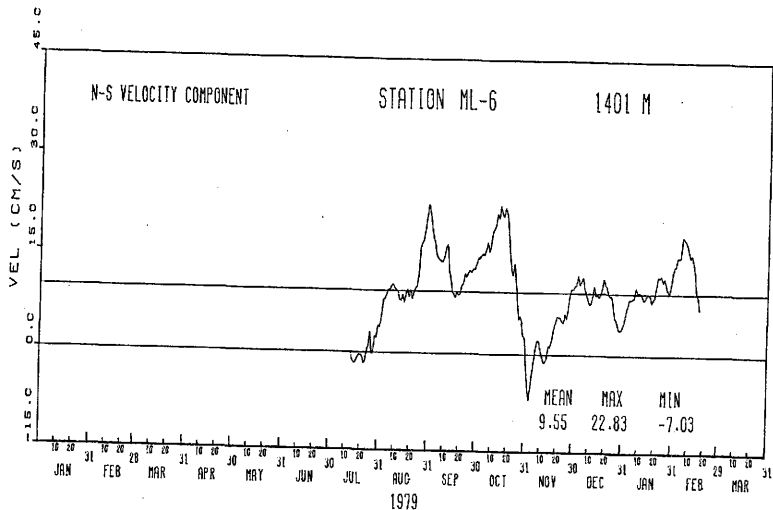


Fig. 10.a. Daily values of meridional velocity component for the second part of the record from the intermediate depth meter at ML6.

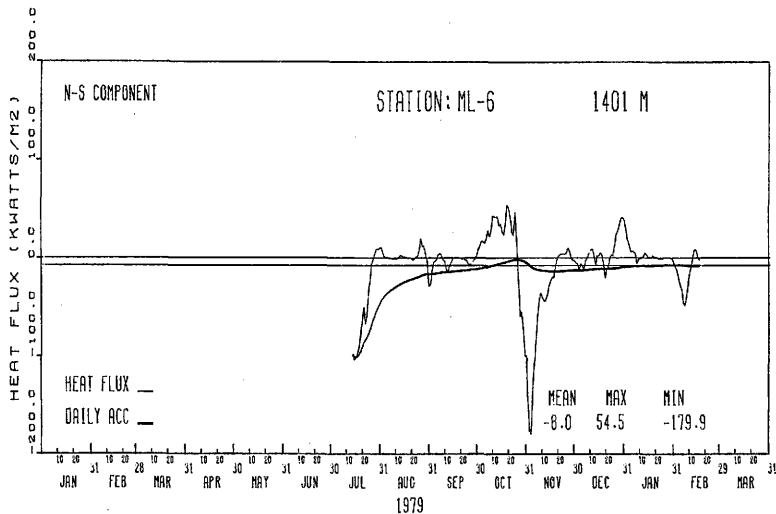


Fig. 10.c. Daily values of meridional eddy heat flux for the second part of the record from the intermediate depth meter at ML6.

The meridional velocity component, temperature and eddy heat flux from the first portion of the ML7 record, extending from early February to late July, are presented in Fig. 11. A poleward mean eddy heat flux is obtained for that period of time. The second part of the record, extending from late July to late December, is presented in Fig. 12. This pictures an equatorward mean eddy heat flux. However, the original equatorward eddy heat flux estimate of 27.4 kWm^{-2} has been reduced by an order of magnitude (to 3.7 kWm^{-2}) for this part of the record. Moreover, examination of the cumulative eddy heat flux curve reveals that the sign of the heat flux is almost entirely determined by a large event in late August. The contribution to mean eddy heat fluxes by events is discussed in the following section.

The sign of the meridional, record-length heat flux also changes from poleward to equatorward near the location of the Continental Water Boundary in the southern Drake Passage. The value from the instrument at 509 m on mooring SS1000 is 26.9 kWm^{-2} equatorward, whereas at the next mooring to the north, ST, the mean eddy heat flux at 695 m is 13.6 kWm^{-2} poleward. Examination of the temperature record at SS1000 (Fig. 13) shows periods at the beginning and end of the record during which the temperature is near 1°C . The mid portion of the record is colder and much more variable. The meridional velocity component from this meter showed variability about zero during the beginning and ending portions of the record and stronger southward flow during the mid record. This combination gives rise to the large equatorward eddy heat flux

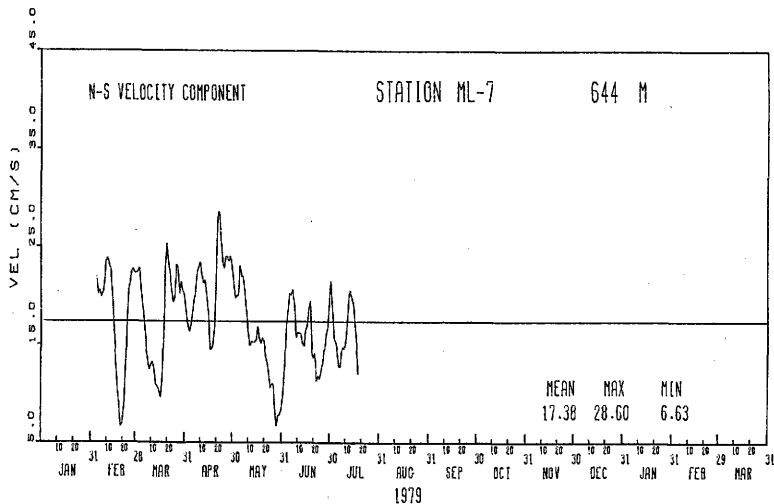


Fig. 11.a. Daily values of meridional velocity component for the first part of the record from the upper meter at ML7.

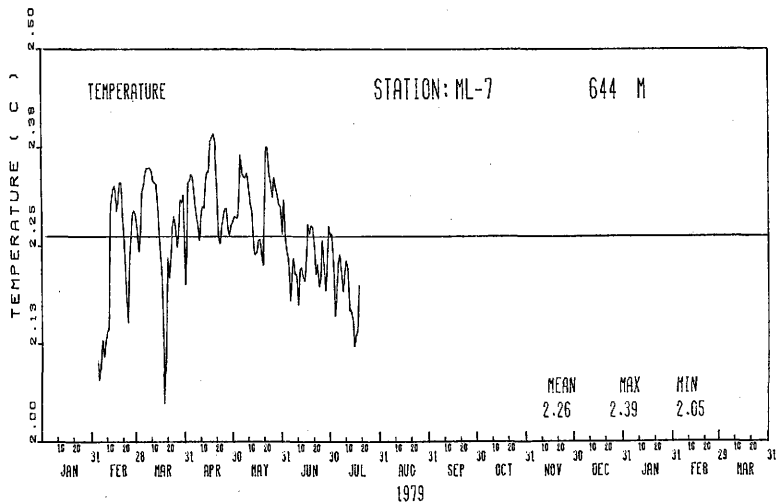


Fig. 11.b. Daily values of temperature for the first part of the record from the upper meter at ML7.

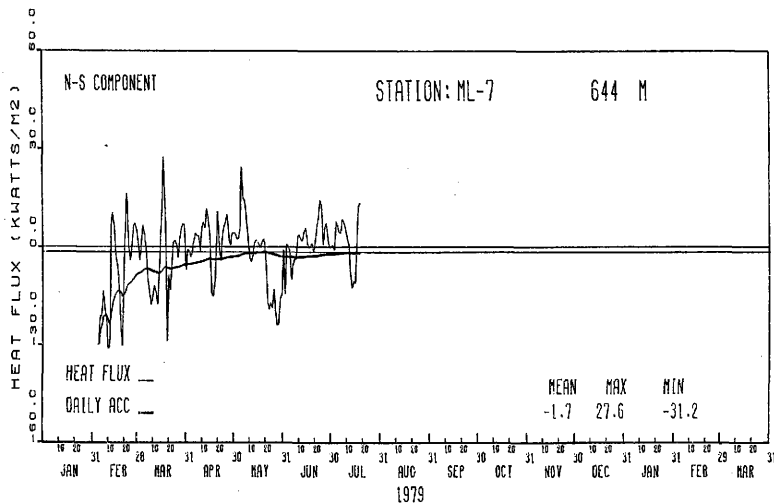


Fig. 11.c. Daily values of meridional eddy heat flux for the first part of the record from the upper meter at ML7.

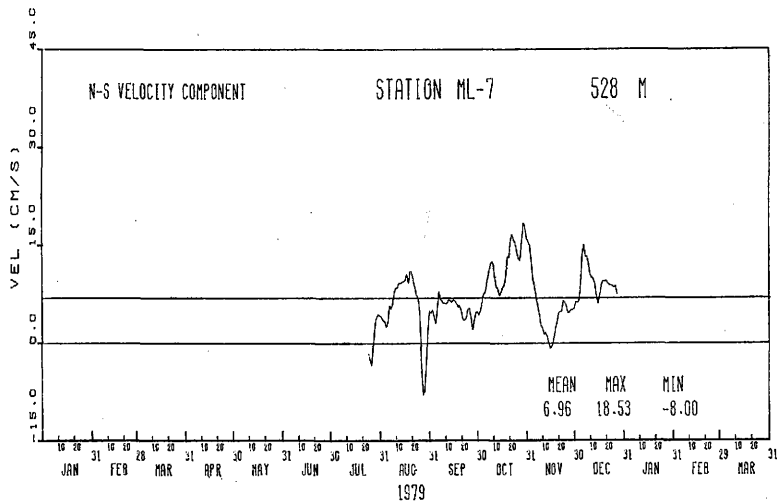


Fig. 12.a. Daily values of meridional velocity component for the second part of the record from the upper meter at ML7.

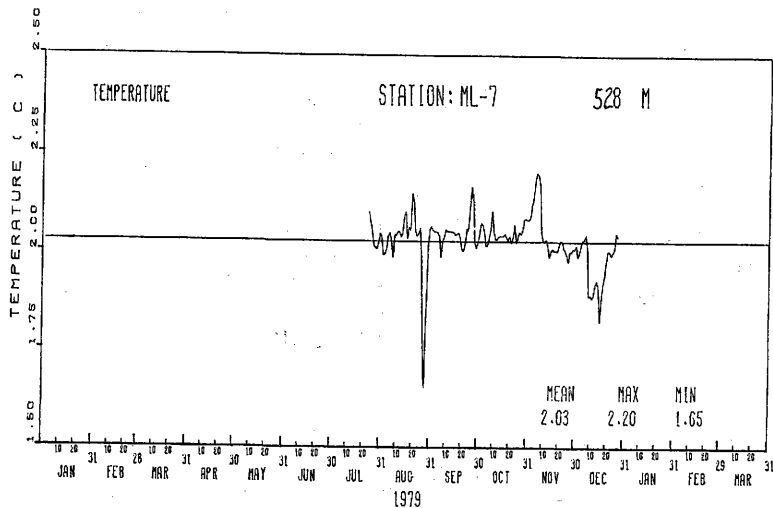


Fig. 12.b. Daily values of temperature for the second part of the record from the upper meter at ML7.

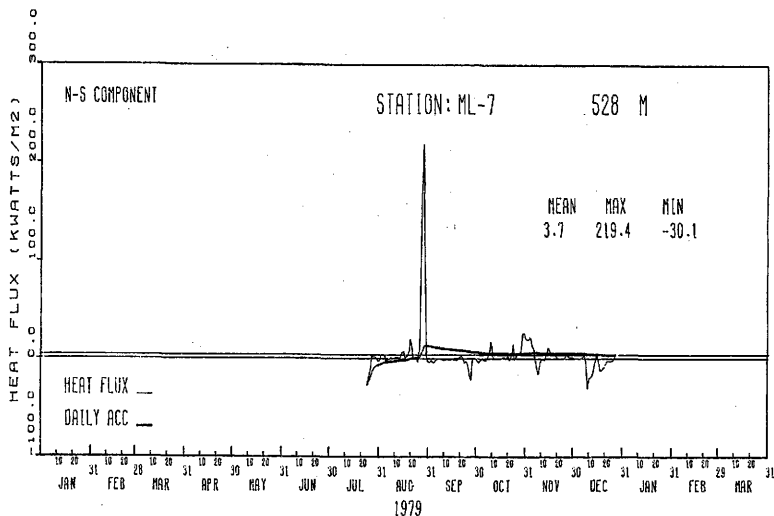


Fig. 12.c. Daily values of meridional eddy heat flux for the second part of the record from the upper meter at ML7.

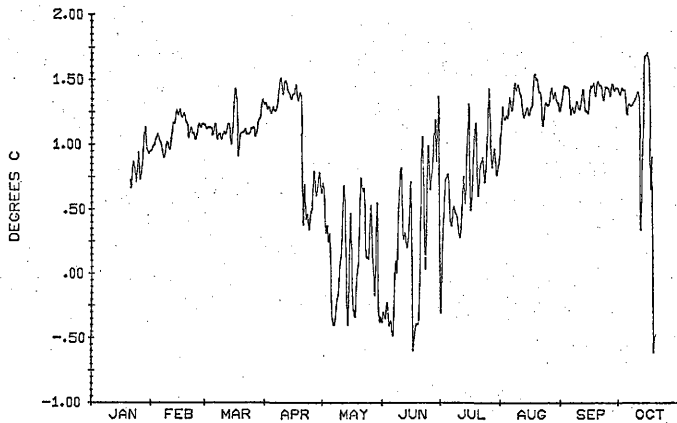


Fig. 13. Temperature at 509 m on Mooring SS1000 during 1979.

when $v'T'$ are calculated relative to their record-length averages. Dividing the record into three portions at April 21 and July 11 and treating each portion as independent records yields mean heat fluxes of 5.0 kWm^{-2} poleward, 2.0 kWm^{-2} equatorward and 0.9 kWm^{-2} poleward for the three portions. However, none of these values differ from zero at the 95% level of significance, though the 5.0 value is significant at the 90% level.

3. Influence of Individual Events

The discrete nature of large contributions to the eddy heat flux at Drake Passage has been stressed by Sciremammano (1980). He found that the mean record-length eddy heat fluxes were dominated by events passing the recording instruments. This same effect is found in DRAKE 79 measurements. For example, most of the equatorward heat flux (3.7 kWm^{-2}) in the second half of the ML7 record (Fig. 12) was contributed by one brief, though strong, event which occurred near the end of August. Removal of that event reduced the record-length eddy heat flux to 0.7 kWm^{-2} equatorward. Moreover, this new value was not significantly different from zero at the 95% level.

In order to assess the significance of the discrete events to the mean heat flux, daily heat flux values were used to obtain a quantitative measure of the contribution by individual events to the mean record-length eddy heat flux. For this purpose, such record of Q_i as a function of time was examined for Q_i values which

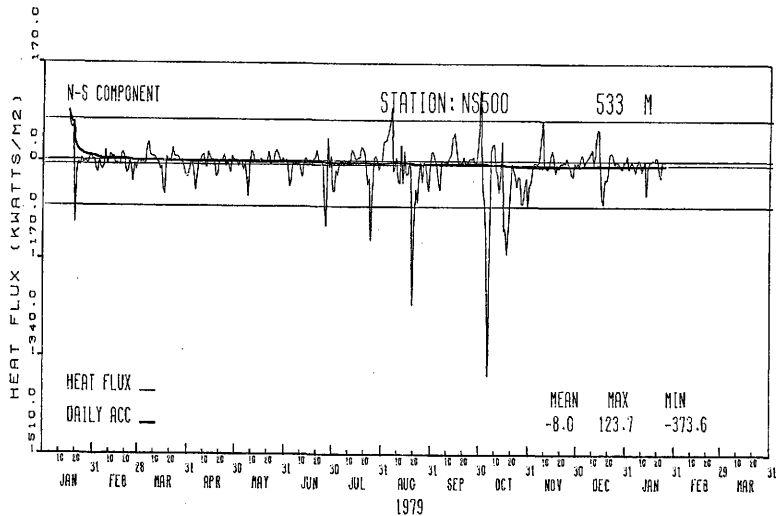


Fig. 14. Daily average, meridional eddy heat flux for the meter at NS500. Horizontal lines are placed 2 standard deviations from record-length eddy heat flux.

departed by more than twice the corresponding standard deviation from the record-length mean eddy heat flux.

As an example, in the heat flux record at NS500 (Fig. 14) we can identify six events. The first major event, occurring for about 6 days during August, accounts for 17% of the total heat flux. The two following events, occurring for five days each during October account for 27% and 19% of the total heat flux respectively. Those three events account for 63% of the total heat flux in less than 5% of its total record length.

Examination of all the individual records shows that individual events contribute more than 50% of the total heat flux in less than 20% of the total record lengths. Events are identifiable throughout the water column at a given mooring (See Appendix Figs. A.3, A.6, A.7, A.8, A.11, A.16, A.17, A.20, A.21 and A.22). In most cases the event is recorded first at the deepest meter and later at the upper meters. Since most of the examples come from the center of the Passage, those events are related to the lateral migrations of the Polar Front in the form of meanders or detached rings and the upward propagation seen in the figures could be evidence for tilting of the Polar Front.

As an example of a well identified event contributing to the eddy heat flux during DRAKE 79, the passing of a cold-core cyclonic ring over the NT mooring in early 1979 was examined. This ring has been documented elsewhere (Peterson et al., 1981). In essence, the ring resulted from rapid growth of a large meander at the Polar Front

which then pinched off and migrated northeastward. By the end of the cruise the ring seemed to be moving through the Subantarctic Front. Using temperature data from the thermistor chains on mooring NT, it was possible to obtain a temperature time series at a constant depth, eliminating spurious temperature variations caused by mooring blow-over. Thus, a good estimate of the heat flux due to this event was obtained.

Time series for eddy heat flux for the uppermost meter at mooring NT are shown in Fig. 15. The record-length average depth of the meter was 647 m. Figures 15a and 15b show, respectively, the heat flux calculated from the original uncorrected records and from the original velocity records together with the time series of T at 647 m constructed from thermistor chain data. Also shown are time series of heat flux for that portion of the record after the ring had passed the mooring. Figure 15c was obtained from uncorrected records for which the mean depth was 628 m. Figure 15d was obtained using a temperature time series constructed from thermistor chain data at 628 m.

Table 4 presents some results from the detailed analysis of temperature and eddy heat fluxes for the four cases shown in Fig. 15. The percentages of the total record-length in which the fluctuation temperature T' is negative and the eddy heat flux $v'T'$ is poleward are also given. Removing the blow-over from original time series (Figs. 15a and 15c) produces the expected effect, i.e., the mean

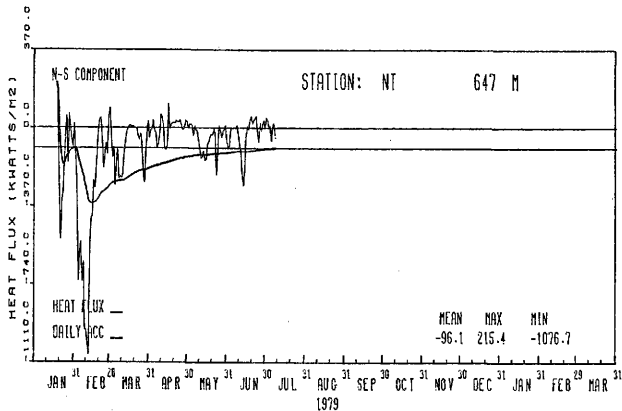


Fig. 15.a. Daily values of meridional eddy heat flux for the uppermost meter at mooring NT from original time series for entire record length. Heavy curve shows cumulative mean eddy heat flux.

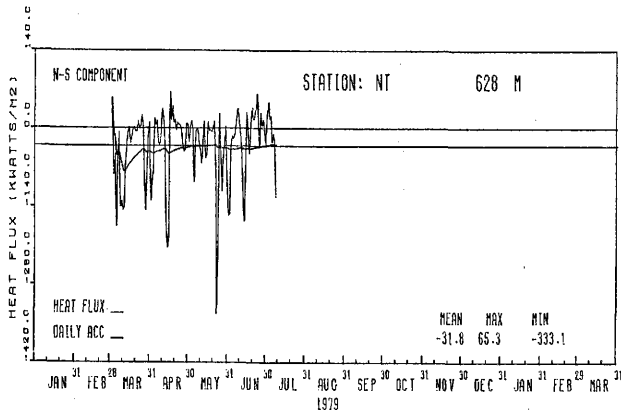


Fig. 15.b. Daily values of meridional eddy heat flux for the uppermost meter at NT using temperature time series at 647 m constructed from thermistor chain data to correct for mooring blow-over. Heavy curve shows cumulative mean eddy heat flux.

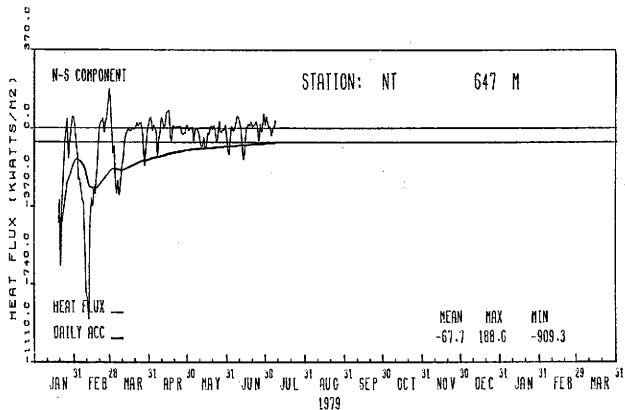


Fig. 15.c. Daily values of meridional eddy heat flux for the uppermost meter at mooring NT from original time series with portion containing ring passage removed. Heavy curve shows cumulative mean eddy heat flux.

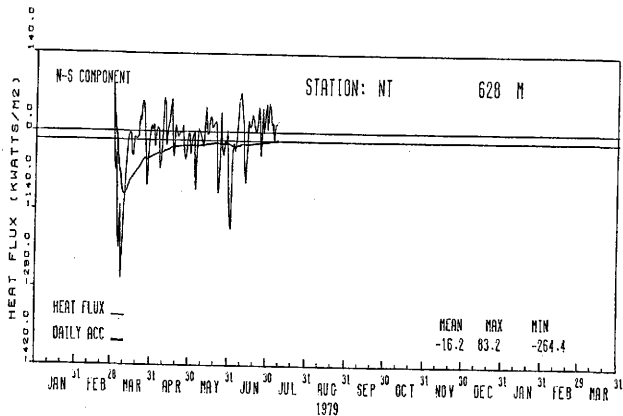


Fig. 15.d. Daily values of meridional eddy heat flux for the uppermost meter at mooring NT from time series with portion containing ring passage removed and corrected in temperature for mooring blow-over. Heavy curve shows cumulative mean eddy heat flux.

Table 4. Results from analysis of temperature and eddy heat flux for the uppermost meter at NT mooring shown in Fig. 6. \bar{T} and \bar{Q} are the record-length mean temperature and eddy heat flux for each case. T' is fluctuation temperature.

| Figure | \bar{T} ($^{\circ}\text{C}$) | \bar{Q} (kWm^{-2}) | % of days when $T' < 0$ | % of days when $v'T' < 0$ |
|--------|-------------------------------------|------------------------------------|----------------------------|------------------------------|
| 15a | 4.26 | -96.1 | 35 | 64 |
| 15b | 4.27 | -67.7 | 38 | 59 |
| 15c | 4.35 | -31.8 | 47 | 62 |
| 15d | 4.37 | -16.2 | 49 | 55 |

temperature \bar{T} is slightly increased. As a consequence, the percentage of days in which the eddy heat flux is poleward is decreased. These changes, though small, produce reductions in the mean record-length eddy heat flux of 30% and 49% for the cases with and without the ring. Removing the ring produces an even greater reduction in poleward eddy heat flux. The original poleward flux of 96.1 kWm^{-2} is reduced 65% to 31.8 kWm^{-2} in the uncorrected records. In the corrected records, this ring accounts for 76% of the total mean eddy heat flux in just 24% of the total record length.

The effect of this ring is also seen in the time required for the cumulative flux to approach the mean values. The time series containing the effects of the ring (Figs. 15a, 15b) must be averaged over five months before the mean is attained while series without the ring approach the mean after only two months.

During 1979, in the northern Drake Passage the time variations of temperature and velocity do not appear to have been greatly affected by frontal shifts of long duration (Fig. 6). In Figs. 16 and 17 are shown time series of v , T and Q_1 from 949 m at NT and 810 m at ML1. These illustrate records in which the fluctuations are dominated by mesoscale events--perhaps rings as discussed by Bryden (1981) or perhaps quasi-periodic wave motions and eddies produced by bottom-current interaction in that area (Klinck, 1981). These records show poleward heat flux.

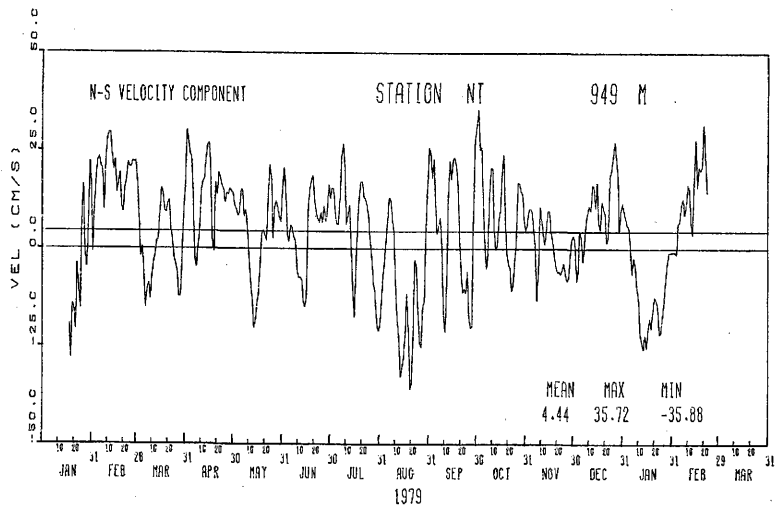


Fig. 16.a. Daily values of meridional velocity component for mooring NT at 949 m.

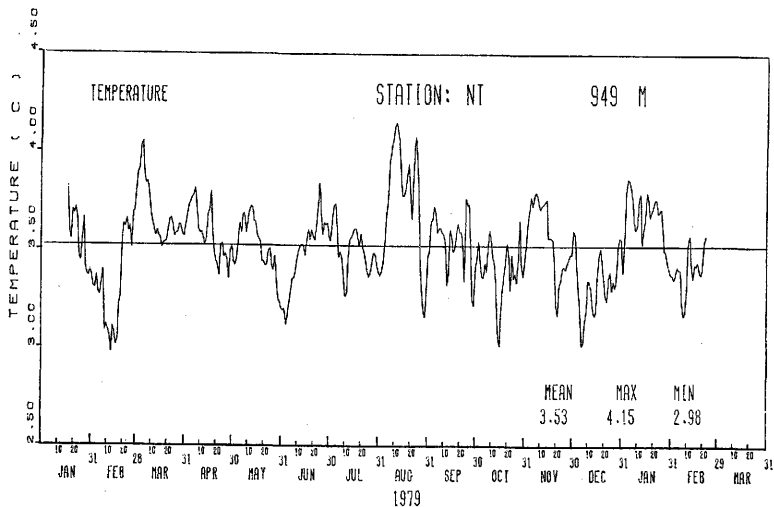


Fig. 16.b. Daily values of temperature for mooring NT at 949 m.

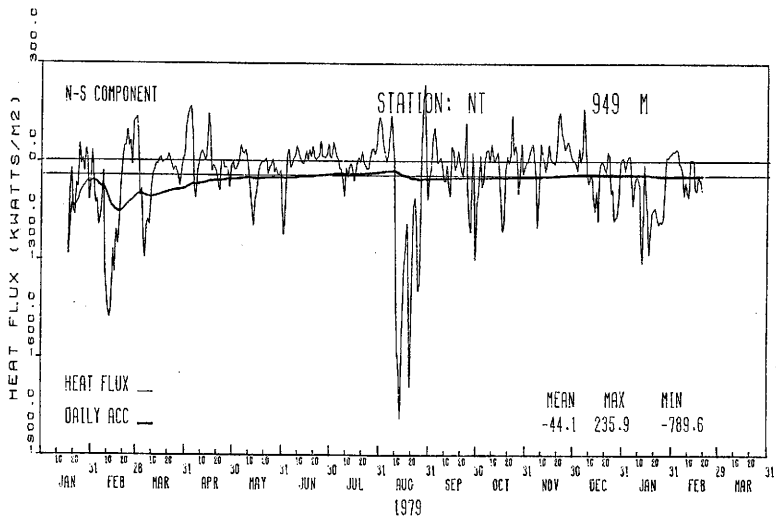


Fig. 16.c. Daily values of meridional eddy heat flux for mooring NT at 949 m.

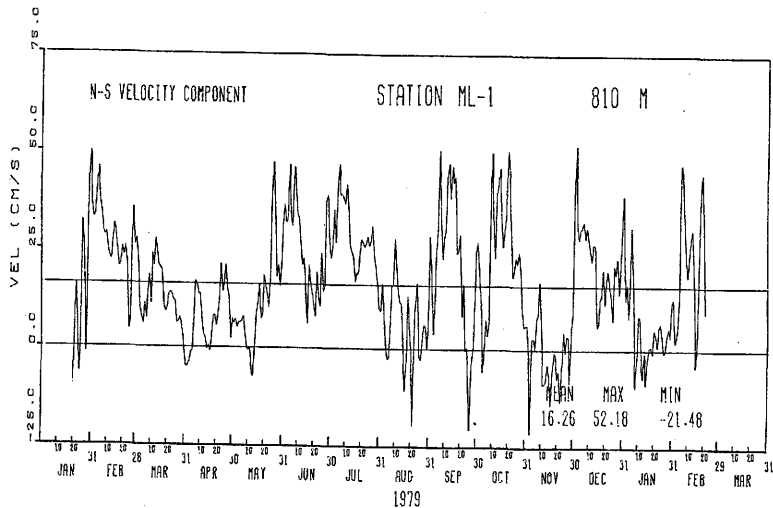


Fig. 17.a. Daily values of meridional velocity component for mooring ML1 at 810 m.

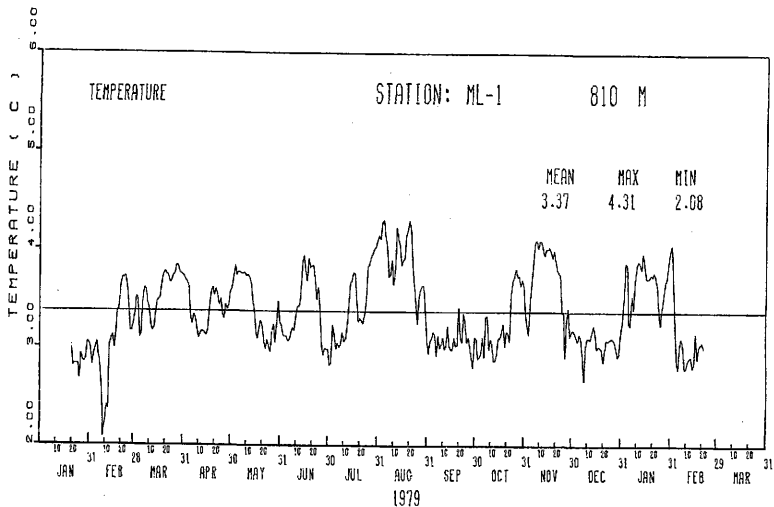


Fig. 17.b. Daily values of temperature for mooring ML1 at 810 m.

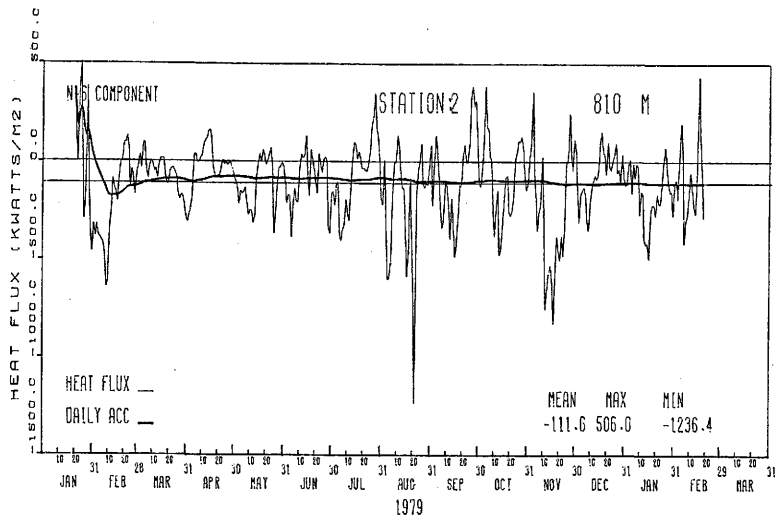


Fig. 17.c. Daily values of meridional eddy heat flux for mooring ML1 at 810 m.

SUMMARY AND CONCLUSIONS

Heat balance estimates indicate that the ocean must transfer heat towards the poles to supply heat lost to the atmosphere at high latitudes. Eddy heat flux, which is a turbulent transfer of heat due to correlated fluctuations of temperature and speed, is suspected to be an important mechanism for the oceanic heat transport. In this study the meridional eddy heat flux due to low-frequency motions in the Antarctic Circumpolar Current has been examined.

Eddy heat flux measurements are point calculations representing temperature and velocity fluctuations at a fixed instrument location, and extrapolation of point measurements to regions must be done with caution. An attempt has been made to preserve more carefully the point nature of the calculations by removing those temperature fluctuations which are due to vertical excursions of the instruments as the moorings blow over during periods of large currents. For one mooring, NT, which was heavily instrumented with thermistor chains above and below the uppermost current meter, it was possible to construct a time series of temperature at a fixed depth. It was found that the eddy heat flux using this corrected time series was 30% less than that calculated from the temperature time series which included vertical excursions. It was concluded that the contamination of temperature measurements by blow-over could seriously bias heat flux estimates from the "soft" moorings used

in the ISOS experiments. The temperature records from other instruments which also had pressure records were corrected using historical vertical temperature gradients to remove the effects of blow-over. Although there are errors associated with the method, it is believed that the resulting heat flux estimates are more representative of the actual values than could be provided by uncorrected measurements. It is also believed that the eddy heat flux estimates in this study are more accurate than those from previous calculations in Drake Passage which have not included corrections for mooring blow-over.

This investigation has also shown that, even though the time series of temperature and velocity are corrected for mooring motions or other sources of bias, care must be taken in constructing and interpreting eddy heat flux means. The character of the time series which constitute the calculations must be evaluated to insure that long-term trends in the data do not result in violations of our assumptions about the time scales being considered. Not only must we filter high frequency fluctuations from the records, but we must remove fluctuations at periods longer than those we consider appropriate for estimates of low frequency turbulence. It has been shown that an annual signal in temperature and velocity at several central Passage moorings resulted in spurious estimates of equatorward heat flux and over-estimates of poleward heat flux at several moorings. Such annual signals are not unique to the

DRAKE 79 measurements, and previous ISOS eddy heat flux estimates are doubtless influenced to some extent by long-period temperature and velocity signals.

Sciremammano (1980) noticed the large contribution of discrete events to the eddy heat flux calculations at Drake Passage. The present study also finds that for most records, more than 50% of the total heat flux is associated with discrete events which occur in time periods less than 20% of the total record length. Our instrumental sampling of Drake Passage has neither the resolution nor coverage necessary to determine whether there are preferred sites for discrete events such as frontal meanders or rings. The large contribution by events to the eddy heat flux may mean that our measurements are more influenced by factors that control meandering and ring translation (e.g., local bathymetry) than by the circum-polar requirement that heat be transported poleward by the ocean.

With the preceding cautions in mind, we may review the current results with those of previous investigators. The average eddy heat flux for the six deep recorders on the Main Line is 4.8 kWm^{-2} poleward. This value incorporates the temperature correction for blow-over, but not an adjustment to remove the effects of the annual temperature signal for central Passage moorings. Were the effect of the frontal shift removed, the mean would not be much affected. The effects of long-term frontal shifts on heat flux means from very deep recorders is less than from the upper recorders. Moreover, we have seen that for the upper meters on ML6

and ML7 compensating for the frontal motion reduces both equatorward and poleward heat fluxes which would tend to preserve the mean value. The heat flux of 4.8 kWm^{-2} is in good agreement with a similar estimate by Bryden (1979) for 1975 data of 6.7 kWm^{-2} .

A subset of the 1979 data from the central Passage can be compared to the estimate of Sciremammano (1980). His value of 17 kWm^{-2} is much larger than our estimate of 2.2 kWm^{-2} . Although part of the difference can be attributed to our correction for blow-over, most of the discrepancy is likely due to inter-annual variability in the position of the Polar Front.

In spite of the uncertainties involved in eddy heat flux measurements and the influence of long period shifts in frontal locations and individual events, it is believed that the estimate of about 5 kWm^{-2} is reasonably accurate, at least for the deep waters of Drake Passage. We are not confident, however, that this estimate can be extrapolated to be representative of the entire Circumpolar Current. The large range of values in the central Passage region illustrates the spatial variability of heat flux estimates and their dependence on external factors.

REFERENCES

- Bryden, H. L., 1979: Poleward heat flux and conversion of available potential energy in Drake Passage. *J. Mar. Res.*, 37, 1-22.
- _____, 1981: The Southern Ocean. Chapter 14 of *Eddies in the Ocean*, A. R. Robinson, Editor. Scientific Committee for Oceanic Research, Paris.
- deSzoeko, R. A. and M. D. Levine, 1981: The advective flux of heat by mean geostrophic motions in the Southern Ocean. *Deep-Sea Res.*, 28, 1057-1085.
- Gordon, A. L., 1975: General Ocean Circulation. In *Numerical Models of Ocean Circulation*, National Academy of Sciences, Washington, 39-53.
- Joyce, T. M. and S. L. Patterson, 1977: Cyclonic ring formation at the Polar Front in the Drake Passage. *Nature*, 265, 131-133.
- _____, W. Zenk and J. M. Toole, 1978: The anatomy of the Antarctic Polar Front in the Drake Passage. *J. Geophys. Res.*, 83, 6093-6113.
- Klinck, J. M., 1981: Flow variability in northern Drake Passage. *Trans. Amer. Geophys. Union*, 62, 924.
- Nowlin, Jr., W. D., T. Whitworth III and R. D. Pillsbury, 1977: Structure and transport of the Antarctic Circumpolar Current at Drake Passage from short-term measurements. *J. Phys. Oceanogr.*, 7, 788-802.
- _____, R. D. Pillsbury and J. Bottero, 1980: Observations of kinetic energy levels in the Antarctic Circumpolar Current at Drake Passage. *Deep-Sea Res.*, 28, 1-17.
- _____, and M. A. Clifford, 1982: The kinematic and thermohaline zonation of the Antarctic Circumpolar Current at Drake Passage. *J. Mar. Res.* (in press).
- Ostle, R. and R. W. Mensing, 1979: *Statistics in Research*. The Iowa State University, Ames, 596 pp.
- Peterson, R. G., W. D. Nowlin, Jr. and T. Whitworth, 1982: Generation and evolution of a cyclonic ring at Drake Passage in early 1979. *J. Phys. Oceanography* (in press).
- Pillsbury, R. D., T. Whitworth III, W. D. Nowlin, Jr. and F. Sciremammano, 1979: Currents and temperatures as observed in Drake Passage during 1975. *J. Phys. Oceanogr.*, 9, 469-482.

- Program Summary of the International Southern Ocean Studies, 1980: National Science Foundation, Washington, D.C. NSF publication 80-4, 213 pp.
- Reynolds, O., 1894: On the dynamical theory of incompressible viscous fluids and the determination of the criterion. *Phil. Trans. Roy. Soc.*, 186, 183.
- Sciremammano, Jr., E., 1980: The nature of the poleward heat flux due to low-frequency current fluctuations in Drake Passage. *J. Phys. Oceanogr.*, 10, 843-852.
- _____, R. D. Pillsbury, W. D. Nowlin, Jr. and T. Whitworth III, 1980: Spatial scales of temperature and flow in Drake Passage. *J. Geophys. Res.*, 85, 4015-4028.
- Trenberth, K. E., 1979: Mean annual poleward transports by the oceans in the Southern Hemisphere. *Dyn. Atm. Ocn.*, 4, 57-64.
- Vonder Haar, T. H. and A. H. Oort, 1973: New estimate of annual poleward energy transport by Northern Hemisphere oceans. *J. Phys. Oceanogr.*, 3, 169-172.
- Whitworth III, T., 1979: Zonation and geostrophic flow at Drake Passage. Ph.D. dissertation, Texas A&M University, College Station, Texas, 79 pp.
- _____, and J. F. Gallo, 1981: Synoptic maps of temperature and flow in Drake Passage: 1979. *Trans. Amer. Geophys. Union*, 62, 924.
- _____, W. D. Nowlin, Jr. and S. J. Worley, 1982: The net transport of the Antarctic Circumpolar Current through Drake Passage. Submitted to *J. Phys. Oceanogr.*

APPENDIX

Time Series of Eddy Heat Fluxes from DRAKE 79 Data

For all long-term records collected during DRAKE 79, time series of eddy heat flux values are presented in this Appendix. In the field, the instruments sampled temperature and velocity every hour. Low-passed records were obtained by applying a cosine-Lanezos filter with a half-power point at 40 h and resampling the filtered data at 6-h intervals. A time series of daily values of temperature (T) and northward component of velocity (v) were obtained by averaging the low-passed, 6-h records. Finally, daily average values of fluctuation temperature (T') and fluctuation northward velocity component (v') were computed relative to record-length means:

$$T' = T - \bar{T},$$

$$v' = v - \bar{v},$$

where \bar{T} and \bar{v} are record-length means of T and v .

Values of northward eddy heat flux for the i th day (Q_i) were computed using

$$Q_i = \bar{\rho} C_p \langle v' T' \rangle,$$

where $\bar{\rho}$ and C_p are the mean density and specific heat at constant pressure of seawater, respectively. The cumulative mean of the eddy heat flux as a function of time was computed, at each time $t = m\Delta t$, using

$$\bar{\rho} C_p m^{-1} \sum_{j=1}^m v'(j\Delta t) T'(j\Delta t),$$

where $v'(j\Delta t)$ and $T'(j\Delta t)$ are fluctuation northward velocity component and temperature at time $j\Delta t$, Δt is the time step equal one day, j is an index of days beginning with the first day of the record and m is the record day for which cumulative heat flux is calculated.

In Figs. A.1 through A.22 are shown plots of time series of Q_i and cumulative heat flux for DRAKE 79 moored instruments from the Main Line (ML) array and the Mapping and Statistics (MS) array.

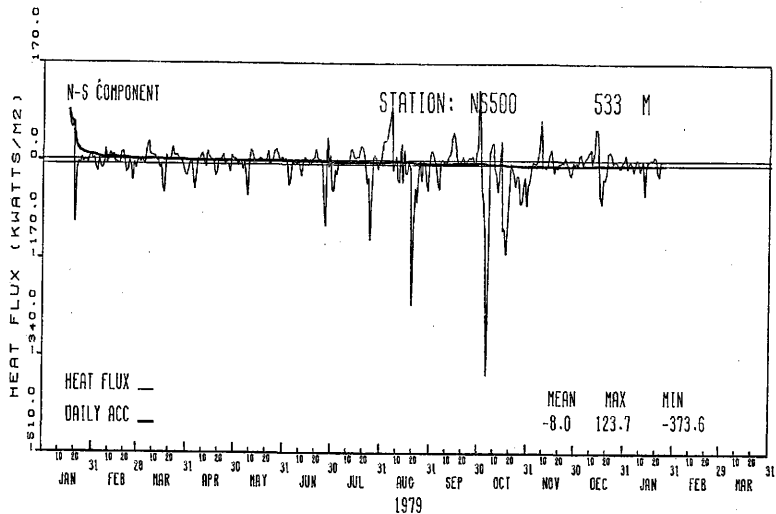


Fig. A.1. Daily average, meridional eddy heat flux for the instrument located at 533 m average depth on mooring NS500. Heavy line is cumulative mean eddy heat flux.

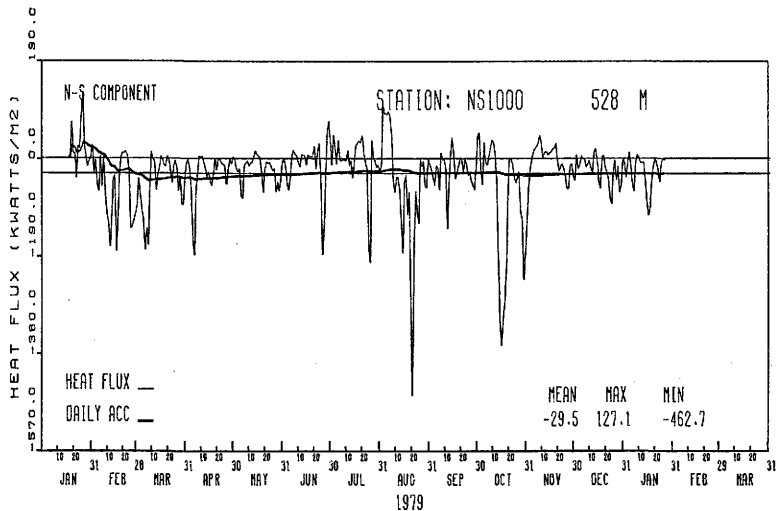


Fig. A.2. Daily average, meridional eddy heat flux for the instrument located at 528 m average depth on mooring NS1000. Heavy line is cumulative eddy heat flux.

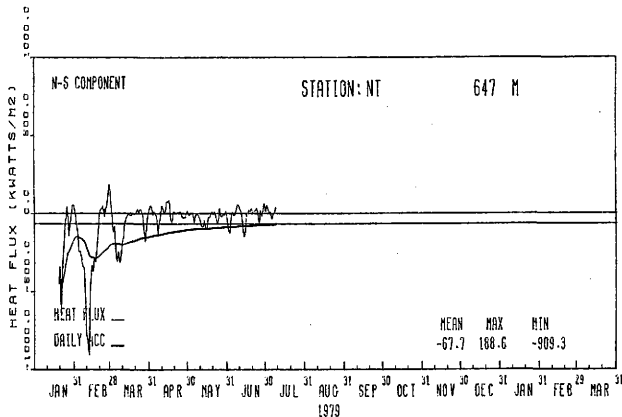


Fig. A.3.a. Daily average, meridional eddy heat flux for the instrument located at 647 m average depth on mooring NT. Heavy line is cumulative eddy heat flux.

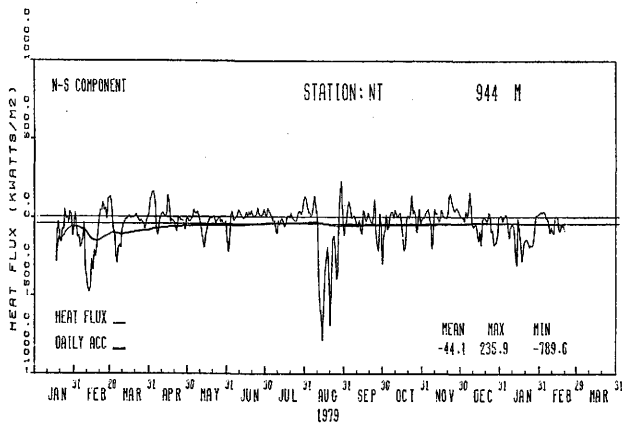


Fig. A.3.b. Daily average, meridional eddy heat flux for the instrument located at 944 m average depth on mooring NT. Heavy line is cumulative eddy heat flux.

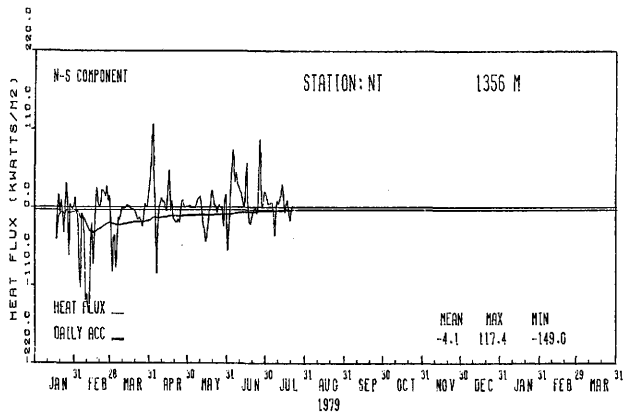


Fig. A.3.c. Daily average, meridional eddy heat flux for the instrument located at 1356 m average length on mooring NT. Heavy line is cumulative eddy heat flux.

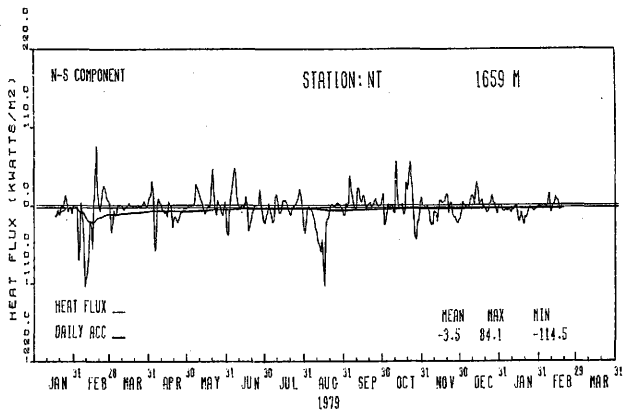


Fig. A.3.d. Daily average, meridional eddy heat flux for the instrument located at 1659 m average depth on mooring NT. Heavy line is cumulative eddy heat flux.

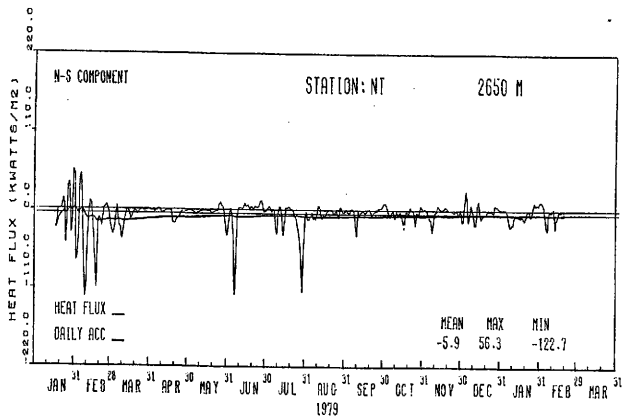


Fig. A.3.e. Daily average, meridional eddy heat flux for the instrument located at 2650 m average depth on mooring NT. Heavy line is cumulative eddy heat flux.

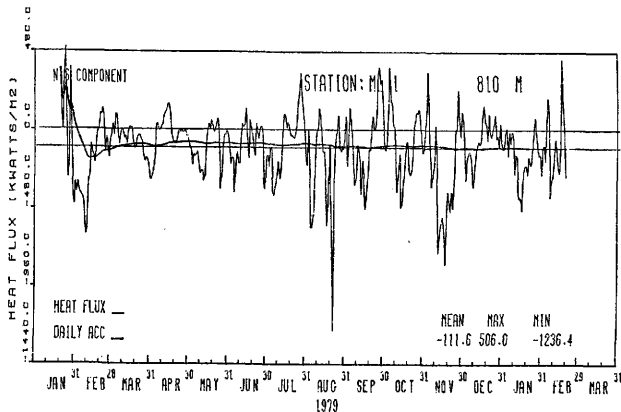


Fig. A.4.a. Daily average, meridional eddy heat flux for the instrument located at 810 m average depth on mooring ML1. Heavy line is cumulative eddy heat flux.

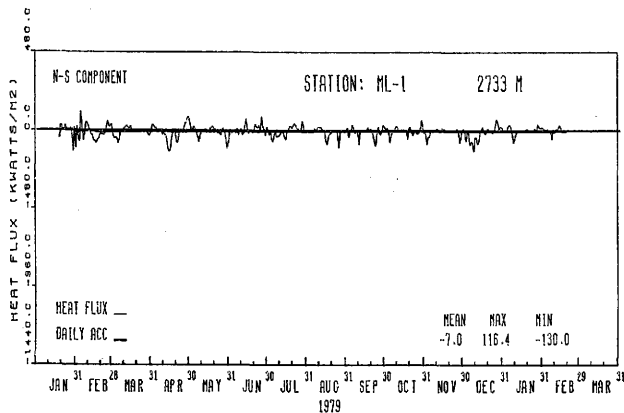


Fig. A.4.b. Daily average, meridional eddy heat flux for the instrument located at 2733 m average depth on mooring ML1. Heavy line is cumulative eddy heat flux.

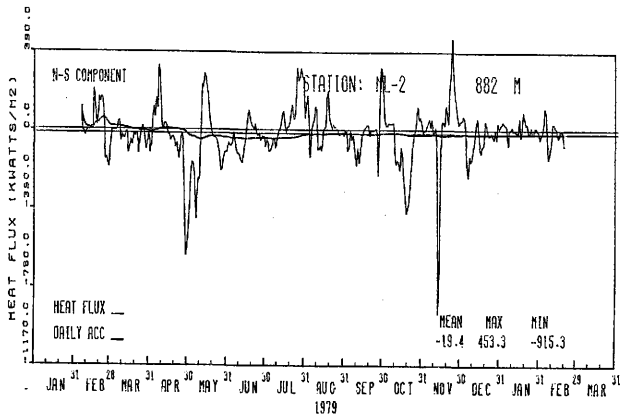


Fig. A.5.a. Daily average, meridional eddy heat flux for the instrument located at 882 m average depth on mooring ML2. Heavy line is cumulative eddy heat flux.

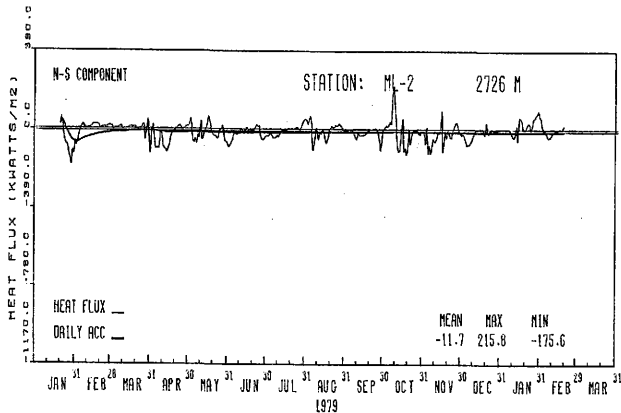


Fig. A.5.b. Daily average, meridional eddy heat flux for the instrument located at 2726 m average depth on mooring ML2. Heavy line is cumulative eddy heat flux.

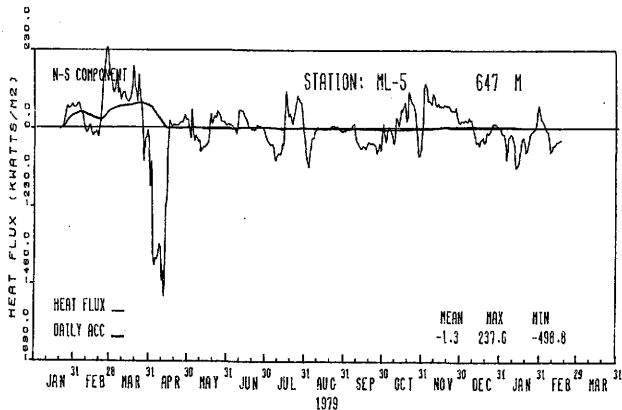


Fig. A.6.a. Daily average, meridional eddy heat flux for the instrument located at 647 m average depth on mooring ML5. Heavy line is cumulative eddy heat flux.

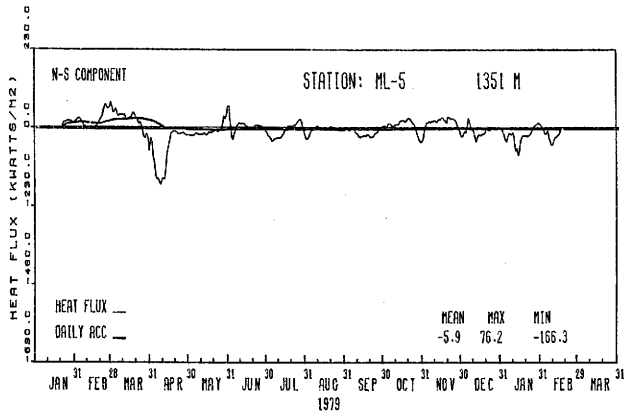


Fig. A.6.b. Daily average, meridional eddy heat flux for the instrument located at 1351 m average depth on mooring ML5. Heavy line is cumulative eddy heat flux.

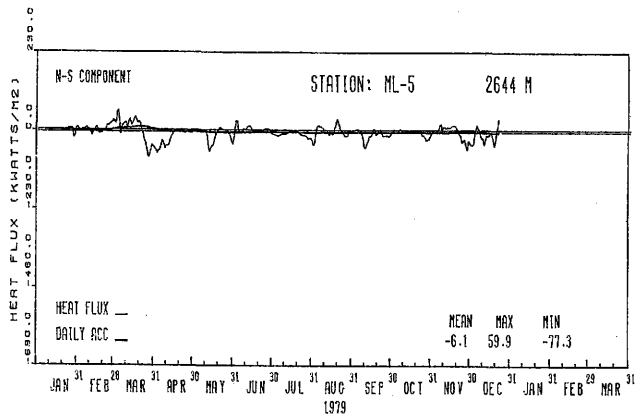


Fig. A.6.c. Daily average, meridional eddy heat flux for the instrument located at 2644 m average depth on mooring ML5. Heavy line is cumulative eddy heat flux.

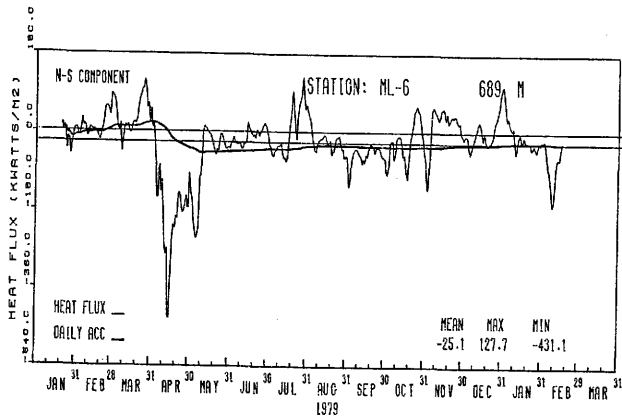


Fig. A.7.a. Daily average, meridional eddy heat flux for the instrument located at 689 m average depth on mooring ML6. Heavy line is cumulative eddy heat flux.

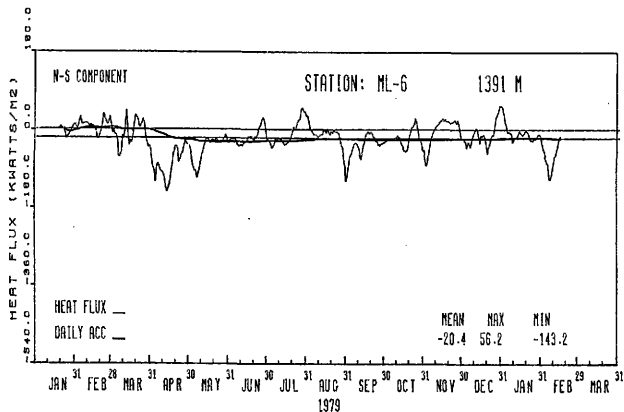


Fig. A.7.b. Daily average, meridional eddy heat flux for the instrument located at 1391 m average depth on mooring ML6. Heavy line is cumulative eddy heat flux.

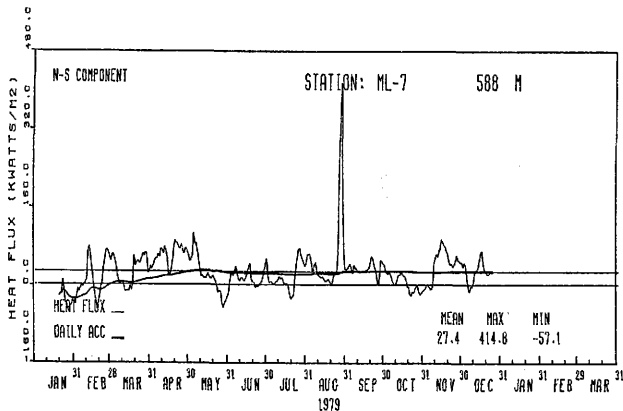


Fig. A.8.a. Daily-average, meridional eddy heat flux for the instrument located at 588 m average depth on mooring ML7. Heavy line is cumulative eddy heat flux.

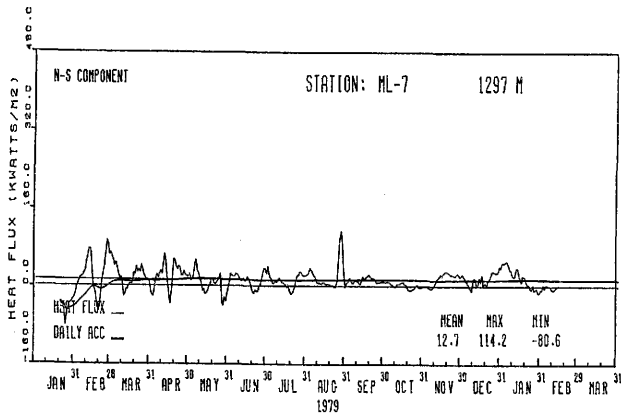


Fig. A.8.b. Daily average, meridional eddy heat flux for the instrument located at 1297 m average depth on mooring ML7. Heavy line is cumulative eddy heat flux.

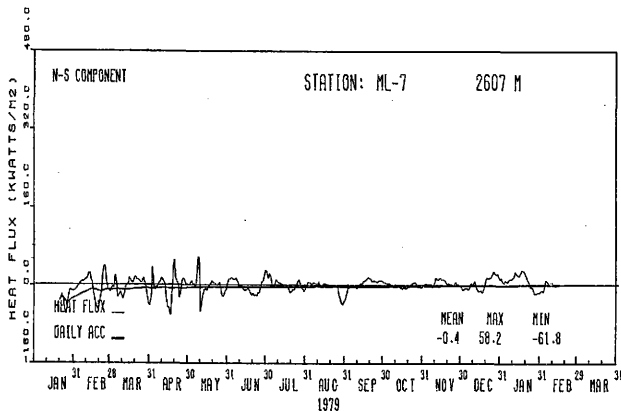


Fig. A.6.c. Daily average, meridional eddy heat flux for the instrument located at 2607 m average depth on mooring ML7. Heavy line is cumulative eddy heat flux.

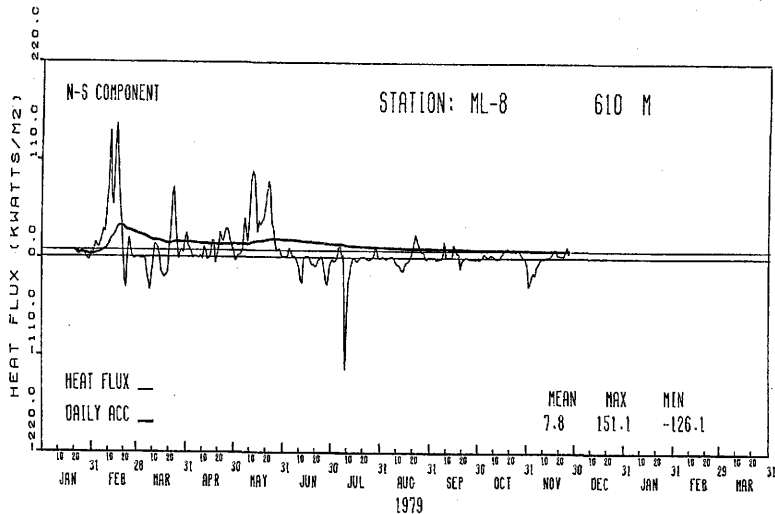


Fig. A.9. Daily average, meridional eddy heat flux for the instrument located at 610 m average depth on mooring ML8. Heavy line is cumulative eddy heat flux.

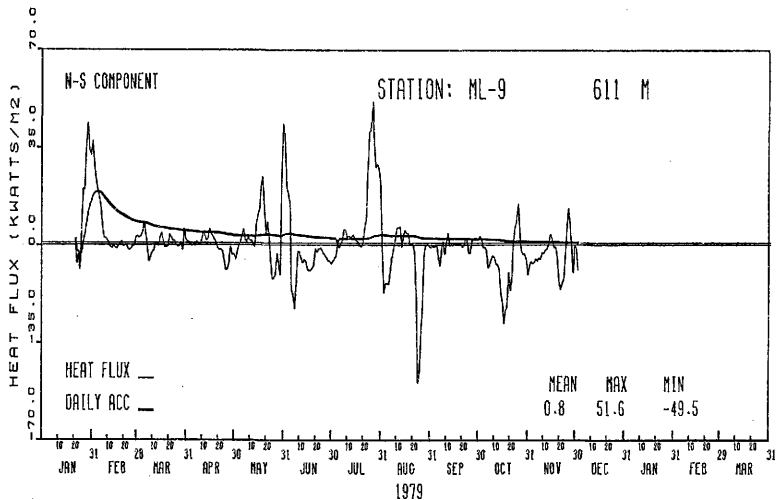


Fig. A.10. Daily average, meridional eddy heat flux for the instrument located at 611 m average depth on mooring ML9. Heavy line is cumulative eddy heat flux.

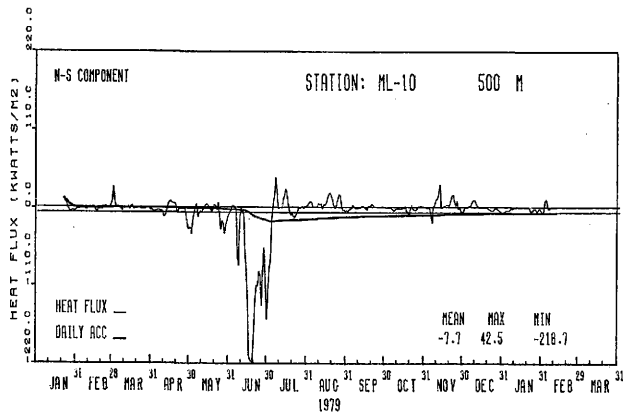


Fig. A.11.a. Daily average, meridional eddy heat flux for the instrument located at 500 m average depth on mooring ML10. Heavy line is cumulative eddy heat flux.

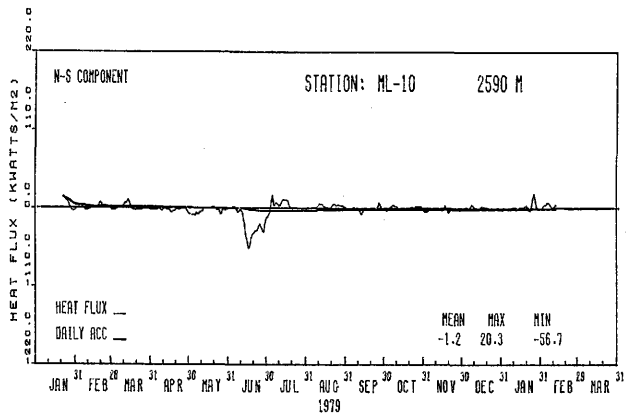


Fig. A.11.b. Daily average, meridional eddy heat flux for the instrument located at 2590 m average depth on mooring ML10. Heavy line is cumulative eddy heat flux.

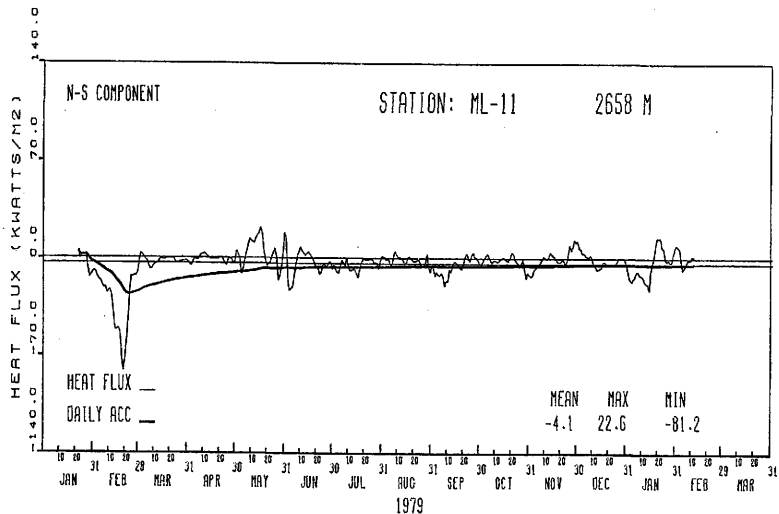


Fig. A.12. Daily average, meridional eddy heat flux for the instrument located at 2658 m average depth on mooring ML11. Heavy line is cumulative eddy heat flux.

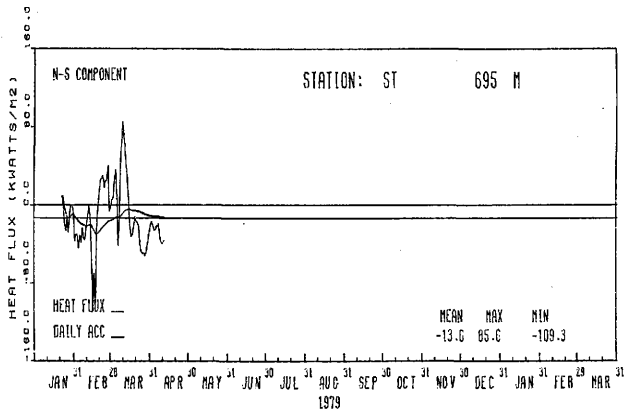


Fig. A.13.a. Daily average, meridional eddy heat flux for the instrument located at 695 m average depth on mooring ST. Heavy line is cumulative eddy heat flux.

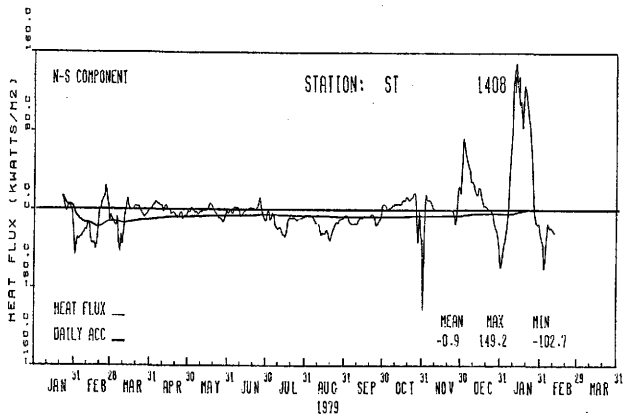


Fig. A.13.b. Daily average, meridional eddy heat flux for the instrument located at 1408 m average depth on mooring ST. Heavy line is cumulative eddy heat flux.

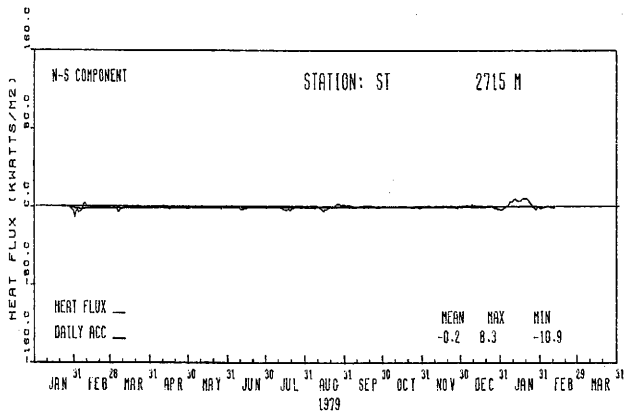


Fig. A.13.c. Daily average, meridional eddy heat flux for the instrument located at 2715 m average depth on mooring ST. Heavy line is cumulative eddy heat flux.

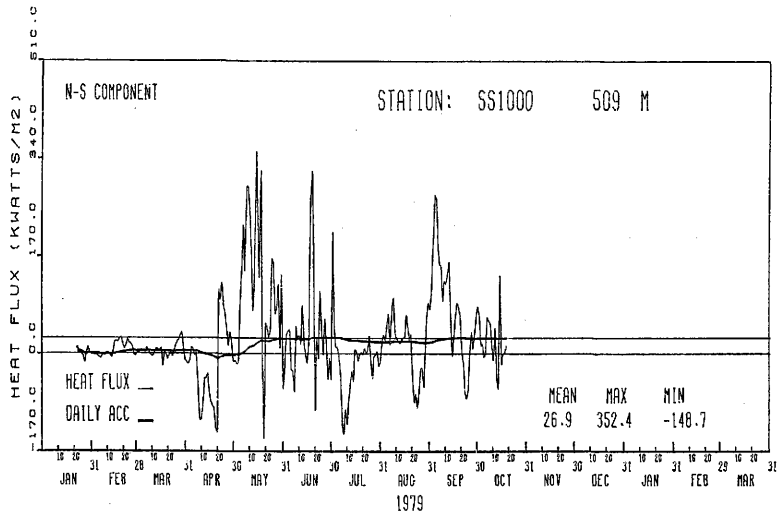


Fig. A.14. Daily average, meridional eddy heat flux for the instrument located at 509 m average depth on mooring SS1000. Heavy line is cumulative eddy heat flux.

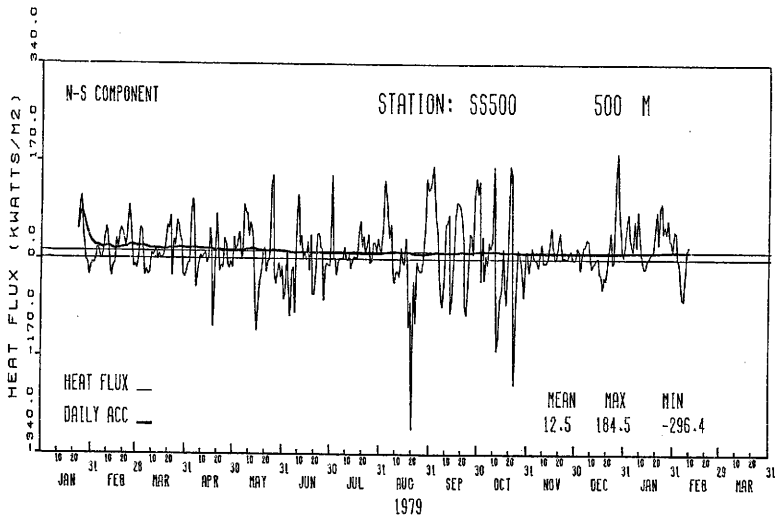


Fig. A.15. Daily average, meridional eddy heat flux for the instrument located at 500 m average depth on mooring SS500. Heavy line is cumulative eddy heat flux.

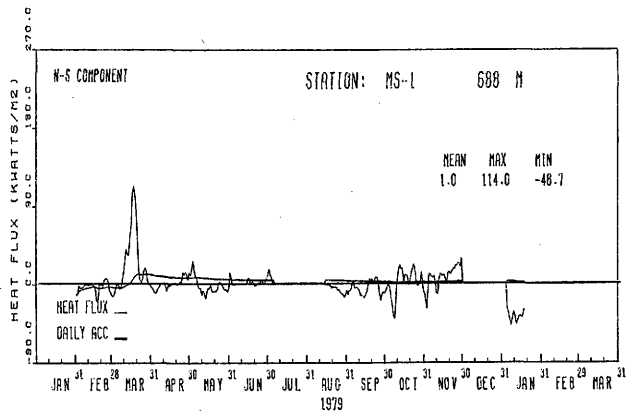


Fig. A.16.a. Daily average, meridional eddy heat flux for the instrument located at 688 m average depth on mooring MS1. Heavy line is cumulative eddy heat flux.

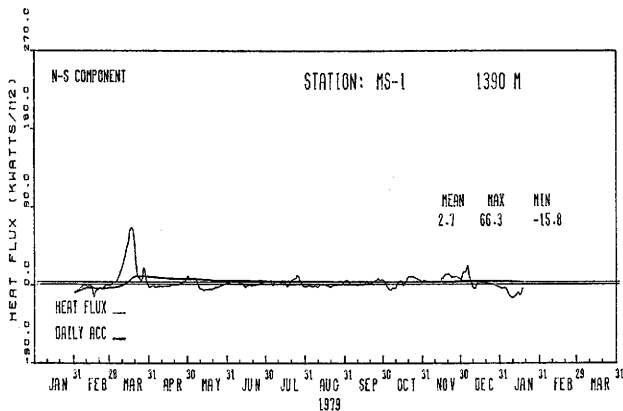


Fig. A.16.b. Daily average, meridional eddy heat flux for the instrument located at 1390 m average depth on mooring MS1. Heavy line is cumulative eddy heat flux.

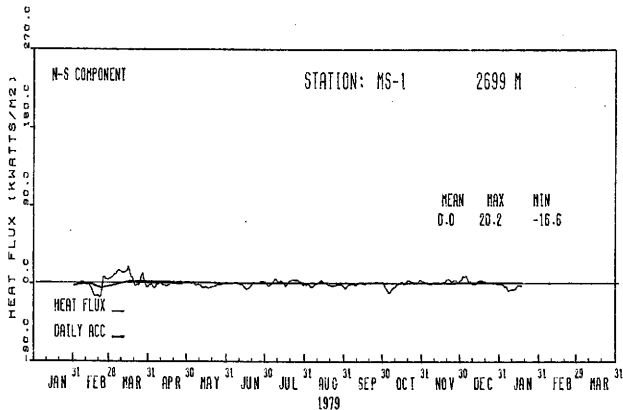


Fig. A.16.c. Daily average, meridional eddy heat flux for the instrument located at 2699 m average depth on mooring MS1. Heavy line is cumulative eddy heat flux.

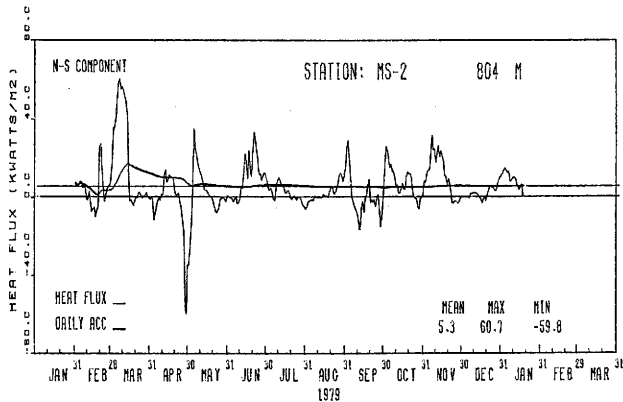


Fig. A.17.a. Daily average, meridional eddy heat flux for the instrument located at 804 m average depth on mooring MS2. Heavy line is cumulative eddy heat flux.

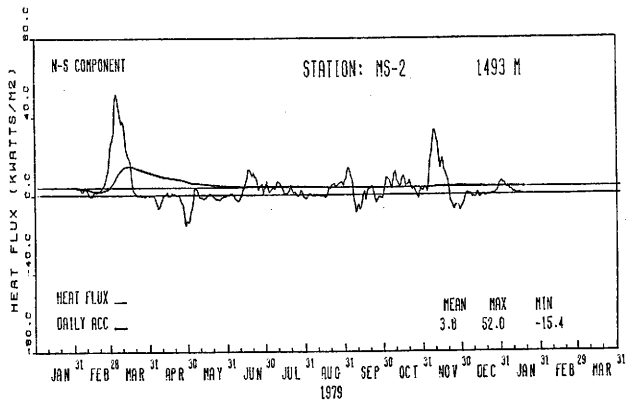


Fig. A.17.b. Daily average, meridional eddy heat flux for the instrument located at 1493 m average depth on mooring MS2. Heavy line is cumulative eddy heat flux.

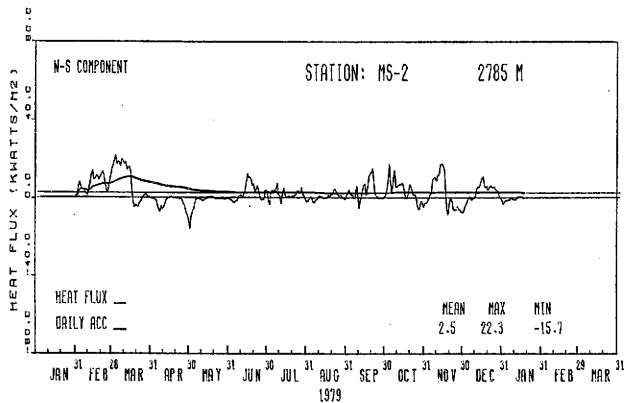


Fig. A.17.c. Daily average, meridional eddy heat flux for the instrument located at 2785 m average depth on mooring MS2. Heavy line is cumulative eddy heat flux.

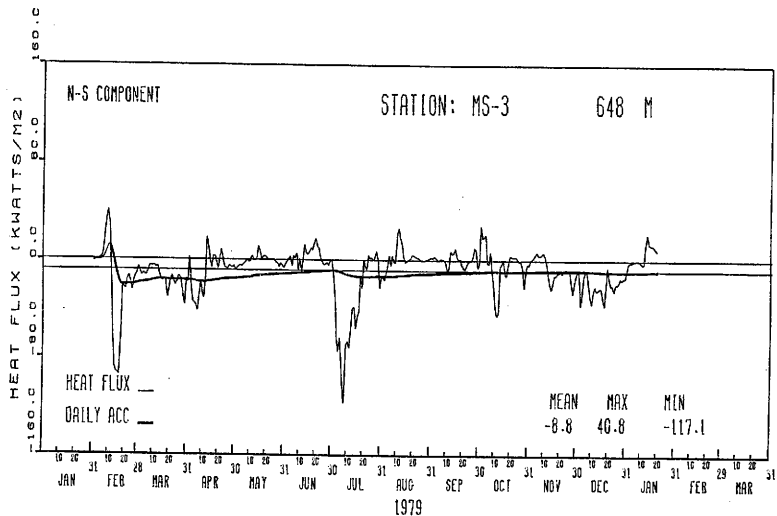


Fig. A.18. Daily average, meridional eddy heat flux for the instrument located at 648 m average depth on mooring MS3. Heavy line is cumulative eddy heat flux.

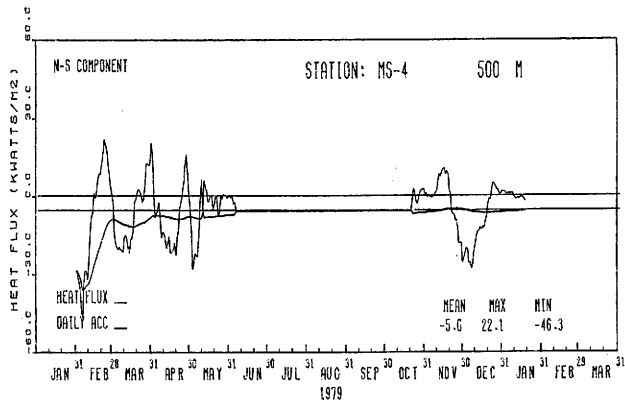


Fig. A.19.a. Daily average, meridional eddy heat flux for the instrument located at 500 m average depth on mooring MS4. Heavy line is cumulative eddy heat flux.

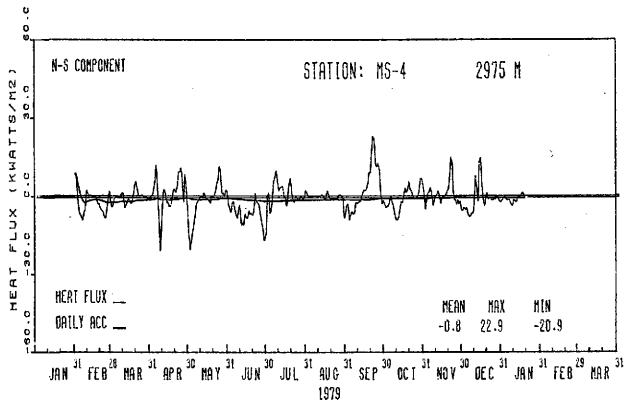


Fig. A.19.b. Daily average, meridional eddy heat flux for the instrument located at 2975 m average depth on mooring MS4. Heavy line is cumulative eddy heat flux.

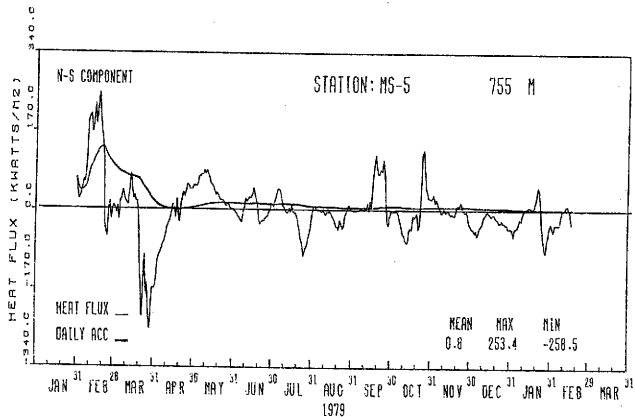


Fig. A.20.a. Daily average, meridional eddy heat flux for the instrument located at 755 m average depth on mooring MS5. Heavy line is cumulative eddy heat flux.

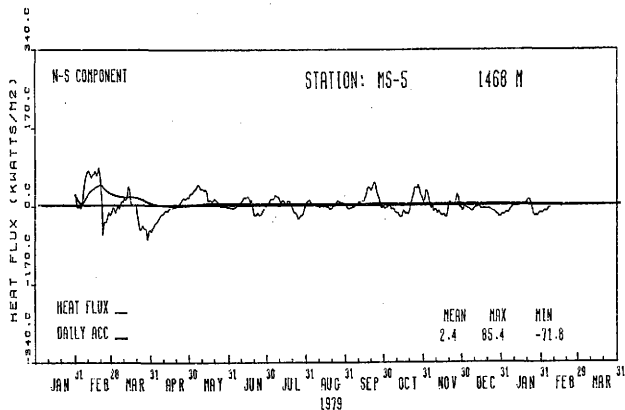


Fig. A.20.b. Daily average, meridional eddy heat flux for the instrument located at 1468 m average depth on mooring MS5. Heavy line is cumulative eddy heat flux.

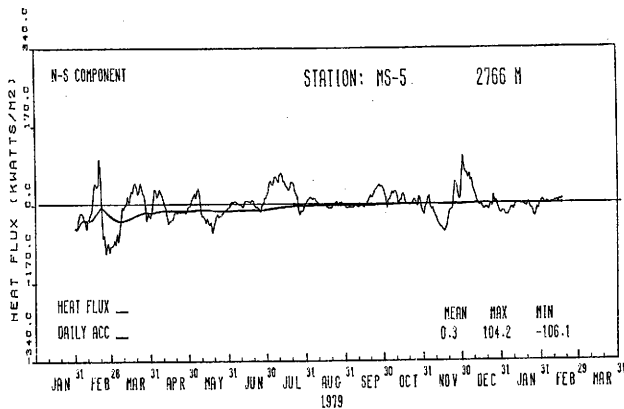


Fig. A.20.c. Daily average, meridional eddy heat flux for the instrument located at 2766 m average depth on mooring MS5. Heavy line is cumulative eddy heat flux.

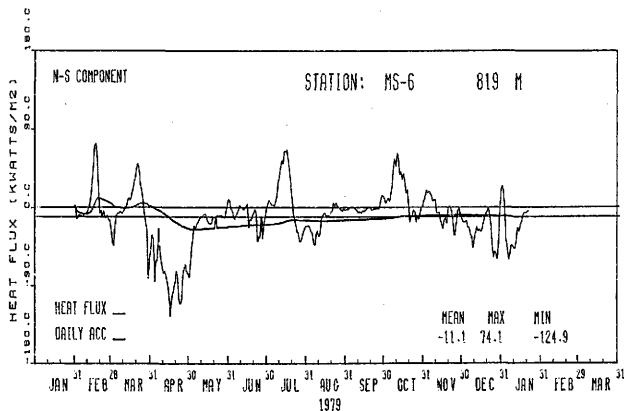


Fig. A.21.a. Daily average, meridional eddy heat flux for the instrument located at 819 m average depth on mooring MS6. Heavy line is cumulative eddy heat flux.

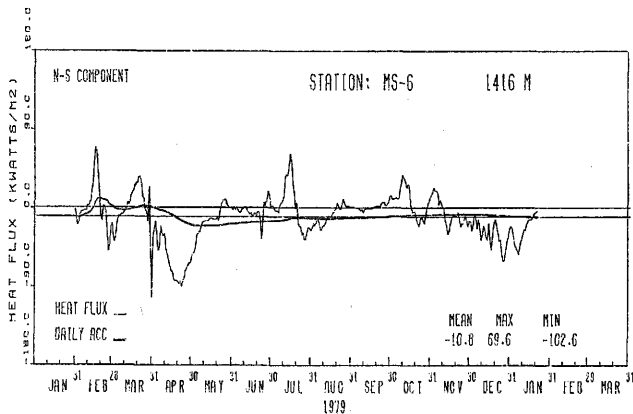


Fig. A.21.b. Daily average, meridional eddy heat flux for the instrument located at 1416 m average depth on mooring MS6. Heavy line is cumulative eddy heat flux.

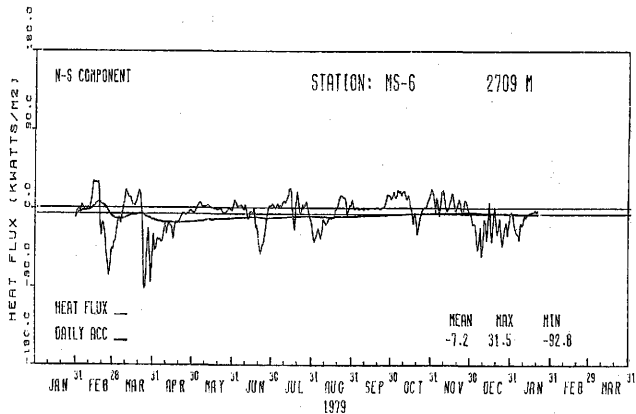


Fig. A.21.c. Daily average, meridional eddy heat flux for the instrument located at 2709 m average depth on mooring MS6. Heavy line is cumulative eddy heat flux.

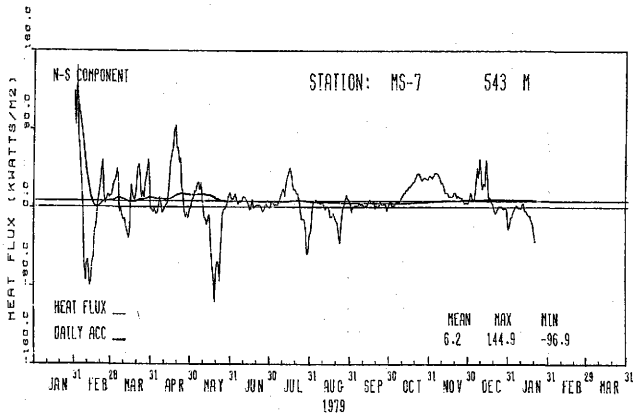


Fig. A.22.a. Daily average, meridional eddy heat flux for the instrument located at 543 m average depth on mooring MS7. Heavy line is cumulative eddy heat flux.

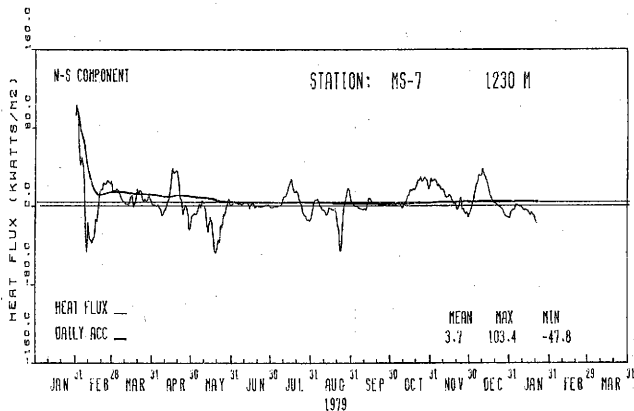


Fig. A.22.b. Daily average, meridional eddy heat flux for the instrument located at 1230 m average depth on mooring MS7. Heavy line is cumulative eddy heat flux.

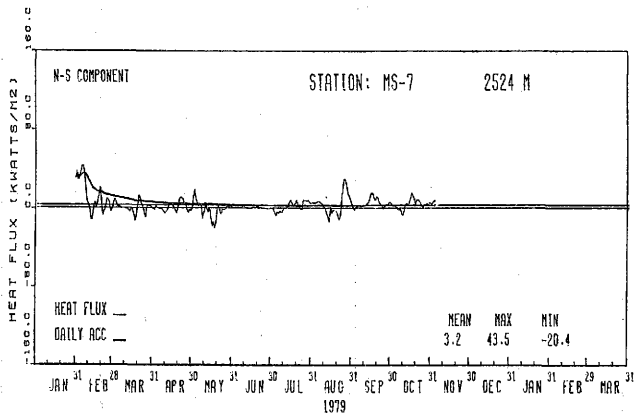


Fig. A.22.c. Daily average, meridional eddy heat flux for the instrument located at 2524 m average depth on mooring MS7. Heavy line is cumulative eddy heat flux.

VITA

Ricardo Luis Rojas Recabal, son of Roberto M. Rojas and Rosa Recabal, was born in Santiago, Chile on January 17, 1953. He graduated from "Manuel Barros Borgono" High School in Santiago, Chile in 1970. From the Catholic University of Valparaiso, Chile he received a Bachelor of Science degree in Physics in 1975.

After graduation, he took a position in the Oceanography Department of the Instituto Hidrografico de la Armada in Valparaiso. In 1976 he began part-time studies in oceanography at the Catholic University of Valparaiso and received the title of Oceanographer in 1977. In that same year he married Emma Rebollo, and in December of 1978 his daughter, Paulina, was born.

With support from the Chilean Navy, Rojas came to Texas A&M University in 1979 and began studies leading to the Master of Science degree in Oceanography. He continues to work for the Chilean Naval Hydrographic Institute where his permanent address is: Instituto Hidrográfico de la Armada, Departamento de Oceanografía, Casilla 324, Valparaíso, Chile.